


ORIGINAL RESEARCH

# Myotubularin-Related Protein14 Prevents Neointima Formation and Vascular Smooth Muscle Cell Proliferation by Inhibiting Polo-Like Kinase1

Ling-Yao Kong , MD, PhD;\* Cui Liang, MD;\* Peng-Cheng Li, MD, PhD;\* Yi-Wei Zhang , MD; Sheng-Dong Feng, MD; Dian-Hong Zhang, MD; Rui Yao, MD, PhD; Lu-Lu Yang, MD; Zheng-Yang Hao, MD; Hao Zhang , MD, PhD; Xiao-Xu Tian, MD; Chen-Ran Guo, MD; Bin-Bin Du, MD; Jian-Zeng Dong , MD, PhD; Yan-Zhou Zhang , MD, PhD

**BACKGROUND:** Restenosis is one of the main bottlenecks in restricting the further development of cardiovascular interventional therapy. New signaling molecules involved in the progress have continuously been discovered; however, the specific molecular mechanisms remain unclear. MTMR14 (myotubularin-related protein 14) is a novel phosphoinositide phosphatase that has a variety of biological functions and is involved in diverse biological processes. However, the role of MTMR14 in vascular biology remains unclear. Herein, we addressed the role of MTMR14 in neointima formation and vascular smooth muscle cell (VSMC) proliferation after vessel injury.

**METHODS AND RESULTS:** Vessel injury models were established using SMC-specific conditional MTMR14-knockout and -transgenic mice. Neointima formation was assessed by histopathological methods, and VSMC proliferation and migration were assessed using fluorescence ubiquitination-based cell cycle indicator, transwell, and scratch wound assay. Neointima formation and the expression of MTMR14 was increased after injury. MTMR14 deficiency accelerated neointima formation and promoted VSMC proliferation after injury, whereas MTMR14 overexpression remarkably attenuated this process. Mechanistically, we demonstrated that MTMR14 suppressed the activation of PLK1 (polo-like kinase 1) by interacting with it, which further leads to the inhibition of the activation of MEK/ERK/AKT (mitogen-activated protein kinase/extracellular-signal-regulated kinase/protein kinase B), thereby inhibiting the proliferation of VSMC from the medial to the intima and thus preventing neointima formation.

**CONCLUSIONS:** MTMR14 prevents neointima formation and VSMC proliferation by inhibiting PLK1. Our findings reveal that MTMR14 serves as an inhibitor of VSMC proliferation and establish a link between MTMR14 and PLK1 in regulating VSMC proliferation. MTMR14 may become a novel potential therapeutic target in the treatment of restenosis.

**Key Words:** MTMR14 ■ neointima formation ■ PLK1 ■ proliferation ■ VSMC

**C**ardiovascular disease is the leading cause of morbidity, mortality, and disability worldwide.<sup>1,2</sup> Atherosclerosis is a chronic progressive

inflammatory disease and a leading cause of cardiovascular diseases. Percutaneous coronary intervention has become one of the main methods for the treatment of

Correspondence to: Yan-Zhou Zhang, MD, PhD, Jian-Zeng Dong, MD, PhD, and Bin-Bin Du, MD, Department of Cardiology, The First Affiliated Hospital of Zhengzhou University, Zhengzhou University, No. 1 Jianshe East Road, Zhengzhou 450052, China. Email: [fcczhangyz@zzu.edu.cn](mailto:fcczhangyz@zzu.edu.cn); [jz\\_dong@126.com](mailto:jz_dong@126.com); [fccubb@zzu.edu.cn](mailto:fccubb@zzu.edu.cn)

\*L.-Y. Kong, C. Liang, and P.-C. Li contributed equally.

Supplemental Material is available at <https://www.ahajournals.org/doi/suppl/10.1161/JAHA.122.026174>

For Sources of Funding and Disclosures, see page 17.

© 2022 The Authors. Published on behalf of the American Heart Association, Inc., by Wiley. This is an open access article under the terms of the [Creative Commons Attribution-NonCommercial-NoDerivs](https://creativecommons.org/licenses/by-nc-nd/4.0/) License, which permits use and distribution in any medium, provided the original work is properly cited, the use is non-commercial and no modifications or adaptations are made.

JAHA is available at: [www.ahajournals.org/journal/jaha](http://www.ahajournals.org/journal/jaha)

## CLINICAL PERSPECTIVE

### What Is New?

- MTMR14 (myotubularin-related protein14) is up-regulated in carotid artery after injury.
- Neointima formation and vascular smooth muscle cell proliferation after vascular injury are mediated by activation of PLK1/MEK/ERK/AKT (polo-like kinase 1/mitogen-activated protein kinase kinase/extracellular-signal-regulated kinase/protein kinase B) signaling pathway.
- MTMR14 inhibits the activation of PLK1/MEK/ERK/AKT axis, thereby inhibiting neointima formation and vascular smooth muscle cell proliferation.

### What Are the Clinical Implications?

- Vascular smooth muscle cell proliferation plays a critical role in the formation of restenosis, and this study demonstrates that MTMR14 suppresses vascular smooth muscle cell proliferation and neointima formation by inhibiting the activation of PLK1/MEK/ERK/AKT signaling pathway, which provides a novel insight into the development of therapeutic strategies for restenosis.

## Nonstandard Abbreviations and Acronyms

|                |  |
|----------------|--|
| <b>CAL</b>     | carotid artery ligation                                |
| <b>FBS</b>     | fetal bovine serum                                     |
| <b>FUCCI</b>   | fluorescence ubiquitination-based cell cycle indicator |
| <b>HE</b>      | hematoxylin–eosin                                      |
| <b>MTM</b>     | myotubularin   |
| <b>MTMR</b>    | myotubularin-related                                   |
| <b>MTMR14</b>  | myotubularin-related protein 14                        |
| <b>PDGF-BB</b> | platelet-derived growth factor BB                      |
| <b>PLK1</b>    | polo-like kinase 1                                     |
| <b>VSMC</b>    | vascular smooth muscle cell                            |

atherosclerotic cardiovascular diseases. However, restenosis is one of the main bottlenecks in restricting the further development of cardiovascular interventional therapy. The specific mechanism and the most appropriate treatment are still the focus of cardiovascular research. Previous studies have reported that the abnormal proliferation of vascular smooth muscle cell (VSMC) plays a vital role in restenosis.<sup>3–5</sup> VSMCs can restore the ability of proliferation from quiescent contractile state in response to vascular injury, resulting in neointima formation and vascular stenosis. The production of proinflammatory mediators that modulate the induction of proliferation and chemotaxis is a feature of this process.<sup>3,4,6</sup> However,

the exact molecular mechanism that underlies neointima formation and VSMC proliferation is unclear.

MTM (myotubularin) and MTMR (myotubularin-related) protein are groups of phosphatases that share a Cys-X5-Arg motif. The catalyzes of these proteins are specifically removing a phosphate group from certain phosphatidylinositol.<sup>7,8</sup> Because phosphatidylinositol acts as an important molecule in a variety of cell processes, MTMR proteins may participate in cell proliferation and differentiation, autophagy, cytokinesis, and cytoskeletal and cell junction dynamics.<sup>7,9</sup> MTMR14 (myotubularin-related protein 14) is a novel phosphoinositide phosphatase conserved through evolution belonging to MTMR family. A previous study revealed that deficiency of MTMR14 promotes cell proliferation in mouse embryonic fibroblasts.<sup>10</sup> In addition, MTMR14 may play a biological role by regulating the star molecule AKT.<sup>11,12</sup> However, the function of MTMR14 in VSMC is less studied.

PLK1 (polo-like kinase1) is a serine/threonine kinase regulating cell cycle progression, which plays a vital role in mitosis.<sup>13</sup> PLK1 is involved in mediating numerous mitotic processes, such as centrosome maturation, regulation of mitotic entry, spindle assembly, chromosome segregation, regulation of G2/M transition, and cytokinesis.<sup>14–21</sup> The activity of PLK1 is upregulated in proliferative cells.<sup>22</sup> The present study suggests that MTMR14 is a novel regulator of VSMC proliferation and neointima formation induced by arterial injury. Moreover, MTMR14 mediates neointima formation and VSMC proliferation by regulating PLK1. The findings provide novel insight into the development of therapeutic strategies for restenosis.

## METHODS

The authors declare that all supporting data are available within the article and its supplemental files.

### Animal Breeding and Genotyping

The animal experiments were performed in accordance with the National Institutes of Health Guidelines for the Care and Use of Laboratory Animals (8th edition, 2011). Moreover, all of the animal protocols were approved by the Ethics Committee of Scientific Research and Clinical Trial of the First Affiliated Hospital of Zhengzhou University.

SMC-specific conditional MTMR14-knockout (*Mtmt14 $\Delta$* ) mice and conditional MTMR14- transgenic (*Mtmt14<sup>TG</sup>*) mice were established through the Cre-loxP system. MTMR14-Flox/Flox mice were generated as described in our previous study.<sup>12</sup> Then, the MTMR14-Flox mice were mated with tamoxifen-inducible transgenic mice ([Myh11-cre/ERT2]1Soff/J) that express CreERT2 driven by the SMC-specific MYH11 promoter

(SMMHC-CreERT2, The Jackson Laboratory, Stock No. 019079) to obtain MTMR14-loxP/loxP-SMMHC-CreERT2 mice. Cre-mediated recombination of the floxed alleles was induced in 6-week-old MTMR14-loxP/loxP-SMMHC-CreERT2 mice through intraperitoneal injections of tamoxifen (1 mg/day, Sigma, T-5648) for 5 consecutive days, leading to the generation of SMC-specific conditional MTMR14-knockout (*Mtmt14 $\Delta$* ) mice. For controls (*Mtmt14<sup>WT</sup>*), littermates, only vehicle was injected. Genotypes were identified as described previously.<sup>12</sup>

The CAG-loxP-stop-loxP-MTMR14 mice were generated as described in our previous study<sup>12</sup> and crossed with SMMHC-CreERT2 transgenic mice to generate CAG-loxP-stop-loxP-MTMR14/SMMHC-CreERT2 mice. Next, 6-week-old CAG-loxP-stop-loxP-MTMR14/SMMHC-CreERT2 mice were injected intraperitoneally with tamoxifen for 5 consecutive days to generate conditional MTMR14-transgenic mice (*Mtmt14<sup>TG</sup>*). MTMR14 expression was evaluated by Western blotting to confirm the SMC-specific MTMR14-transgenic mice were successfully constructed. CAG-loxP-stop-loxP-MTMR14 littermates treated with the same dose of vehicle acted as controls (*Mtmt14<sup>WT</sup>*). Genotypes were identified as described previously.<sup>12</sup>

## Animal Models

Eight-week-old male Sprague–Dawley rats (250–300 g) were used to establish a carotid artery balloon injury model. The rats were anesthetized intraperitoneally with 100 mg/kg ketamine-HCl and 10 mg/kg xylazine-HCl. The left carotid arteries were exposed using blunt dissection, and the distal end of the bifurcation of the external carotid artery was encircled using a 5-0 nylon suture. Then the common carotid artery and the internal carotid artery were clamped with a vascular clip. Next, a small opening was cut in the external carotid artery monitored under a surgical microscope. A balloon catheter measuring 2.0 mm in diameter (Pioneer, Shanghai, China) was inserted into the proximal end of the artery. The balloon was inflated with 0.9% sodium chloride solution and pushed and pulled 10 times within the lumen. Then, the balloon was deflated and removed. Then, we ligated the external carotid artery and opened the internal carotid artery clip, and finally, the wound was sutured. The carotid artery was exposed for the sham injury group, but no damage was performed to the vessels. The animals were allowed to recover and were housed individually under specific pathogen-free conditions with 12/12 hours light/dark cycle (lights on at 6 AM, lights off at 6 PM). The rats were euthanized on the 28th day after the injury, and the left common carotid arteries were removed. Some tissues were subjected to Western blot analysis, some were subjected to quantitative real-time polymerase

chain reaction analysis, others were fixed in paraffin and sliced for hematoxylin–eosin (HE) or immunofluorescence staining.

Eight-week-old male C57BL/6J mice (23–27 g) were used to establish a carotid artery ligation (CAL) model using the same anesthesia protocol described previously. The left carotid arteries were exposed using blunt dissection and ligated using a 6-0 nylon suture; then, the wound was closed. For the sham group, the suture was passed under the exposed carotid artery but not ligated. The animals were allowed to recover and were housed individually under specific pathogen-free conditions with 12/12 hours light/dark cycle (lights on at 6 AM, lights off at 6 PM). For localized adenovirus delivery, Ad-shScramble, Ad-shPLK1, Ad-Control, or Ad-PLK1 ( $4 \times 10^7$  pfu) were packaged by 70  $\mu$ L Pluronic gel F-127 (Keygen, China) to extend virus contact time and delivery to the carotid arteries immediately after ligation respectively. After the mice were euthanized on the 28th day after ligation, the left common carotid arteries were removed, for paraffin embedding, then sliced and subjected to HE or immunofluorescence staining or for protein extraction and molecular biological analyses. (Because of the low amount of protein collected from mouse carotid artery, we mixed carotid arteries from 3 to 4 individuals under equal conditions for the protein extraction.)

## Human Samples

Human specimens were obtained from patients undergoing thigh amputation after femoral artery stenting for restenosis. The samples were obtained from Union Hospital, Tongji Medical College, Huazhong University of Science and Technology. The use of human tissue was approved by medical ethics committee of Union Hospital, Tongji Medical College, Huazhong University of Science and Technology, and all work with human samples conform to the principles outlined in the Declaration of Helsinki. Informed consent was obtained from each patient.

## Cell Culture and Treatment

Mouse VSMCs were isolated from the aortas of 10-week-old C57BL/6J male mice through enzymatic digestion. Blood vessels were removed and washed in PBS, and the fat and connective tissue were stripped away. Then, the isolated aortas were incubated in 1 mL of DMEM containing 3 mg/mL collagenase Type II (C6885, 700.3 U/mg, Sigma) at 37 °C in a humidified chamber for 10 minutes. Then, the aortas were transferred to culture dishes containing 3 mL PBS, and the adventitia was gently removed. Subsequently, the aortas were transferred to culture dishes for incubation overnight with DMEM/F12 medium supplemented with 10% fetal bovine serum (FBS, SV30087.02; HyClone)

and 1% penicillin–streptomycin in a humidified 5% CO<sub>2</sub> atmosphere at 37 °C. The next day, the tissues were minced, transferred to a cell culture flask, and incubated in collagenase Type II and elastase Type I (1 mg/mL, E1250, 6 U/mg, Sigma) for 30 and 60 minutes successively. The collected cells were subsequently cultured in DMEM/F12 medium supplemented with 10% FBS and 1% penicillin–streptomycin in a humidified 5% CO<sub>2</sub> atmosphere at 37 °C. Primary VSMCs between the fourth and sixth passages were used for experiments. HEK 293T cells provided by Procell Biotech (Wuhan, China) were maintained in DMEM supplemented with 10% FBS in a humidified 5% CO<sub>2</sub> atmosphere at 37 °C. Platelet-derived growth factor BB (PDGF-BB) (Sigma, St. Louis, MO) was used in time- and concentration-gradient experiments to determine the final intervention dose. To obtain MTMR14-overexpressing or MTMR14-knockdown cells, recombinant adenovirus containing MTMR14, MTMR14 shRNA (a short hairpin RNA targeting MTMR14), PLK1, and PLK1 shRNA was applied to infect VSMCs *in vitro* or *in vivo*, with the empty vector as a negative control (Ad-Control or Ad-shScramble). For infection, the adenoviruses were used at a multiplicity of 50 particles/cell infection for 24 hour. The cells were used for the indicated analyses and experiments. All adenoviruses were provided by Obio Technology Corp, Ltd. (Shanghai, China).

### Western Blotting

Cells or tissues were homogenized in ice-cold suspension buffer (RIPA Lysis Buffer) supplemented with a proteinase inhibitor cocktail (Sigma-Aldrich). Briefly, the protein concentrations were determined using a bicinchoninic acid protein assay kit (Thermo Scientific, Waltham, MA). Equal amounts of protein were fractionated on (sodium dodecyl sulfate polyacrylamide gels, followed by immunoblotting with the following primary antibodies: anti-MTMR14 (1:1000, Abcam, Catalog No: ab102575)), anti-MTMR11 (1:1000, Sino Biological, Catalog No: 206602-T08), anti-ACTA2 (aortic alpha-actin; 1:1000, Abcam, Catalog No: ab7817), anti-PCNA (1:1000, Abcam, Catalog No: ab29), anti-ERK1/2 (extracellular-signal-regulated kinase; 1:1000, CST, Catalog No: 9102), anti-phospho-ERK1/2 (Thr202/Tyr204) (1:1000, CST, Catalog No: 9106), anti-MEK (mitogen-activated protein kinase; 1:1000, CST, Catalog No: 9126), anti-phospho-MEK (Ser221) (1:2000, CST, Catalog No: 2338), anti-PLK1 (1:1000, CST, Catalog No: 4513), anti-phospho-PLK1(Thr210) (1:1000, CST, Catalog No: 9062), anti-phospho-Akt (Ser473) (1:1000, CST, Catalog No: 4060), anti-AKT (1:1000, CST, Catalog No: 4691), and anti-GAPDH (1:1000, Proteintech, Catalog No: 60004-1-Ig). Membranes were then incubated with a peroxidase-conjugated secondary antibody (horseradish peroxidase-conjugated Affinipure

Goat Anti-Mouse IgG(H+ L)) (1:5000, Proteintech, Catalog No: SA00001-1) or horseradish peroxidase-conjugated Affinipure Goat Anti-Rabbit IgG(H+ L) (1:5000, Proteintech, Catalog No: SA00001-2), and specific bands were detected with a Bio-Rad (Hercules, CA) imaging system. The results were normalized to GAPDH.

### RNA Isolation and Quantitative Real-Time Polymerase Chain Reaction

Total RNA was extracted from cells with TRIzol reagent (D9108A; Takara Bio). Isolated RNA was reverse transcribed into complementary DNA using an RR037A PrimeScript RT reagent Kit (Perfect Real Time) (TaKaRa). SYBR Green (Vazyme) was used to quantify the amplification products on a PRISM 7900 Sequence Detector System (Applied Biosystems, Foster City, CA). 18S was used for normalization. The primers used in the experiment are listed in Table S1.

### Histological, Immunohistochemistry, and Immunofluorescence Analysis

The mice were euthanatized at the indicated times, and the carotid arteries were harvested and fixed with 4% paraformaldehyde before embedding in paraffin. The entire length of the left carotid arteries was sectioned (4 μm) and stained with HE for conventional light microscopic analysis. Five sections located at 250 μm intervals from the carotid bifurcation were examined as described previously.<sup>23</sup>

For immunohistochemistry analysis, after deparaffinization and rehydration with graded ethanol washes, sections were placed in 10 mM Tris-EDTA buffer (pH 9.0) and then samples were heated in a pressure cooker for 20 minutes. After natural cooling to room temperature, the slides were washed in PBS and then incubated with 3% hydrogen peroxide for 10 minutes, washed with PBS, and blocked with 5% normal goat serum for 30 minutes. Next, the sections were incubated with primary antibody anti-MTMR14 (1:200, Abcam, Catalog No: ab102575) at 4 °C overnight, followed by secondary antibody before staining with DAB Kit (ZSGB-BIO, Beijing, China). The nuclei were counterstained with hematoxylin.

For immunofluorescence analysis, after deparaffinization and rehydration with graded ethanol washes, sections were placed in 10 mM Tris-EDTA buffer (pH 9.0) and then samples were heated in a pressure cooker for 20 minutes. After natural cooling to room temperature, the slides were washed in PBS and then blocked with 10% bovine serum albumin for 60 minutes. Next, the sections were incubated with primary antibody at 4 °C overnight. The primary antibodies were as follows: anti-MTMR14 (1:200, Proteintech Catalog

No: 67561-1-Ig), anti-ACTA2 (1:200, Abcam, Catalog No: ab32575), anti-PLK1 (1:100, ABclonal, Catalog No: A2548), anti-phospho-PLK1(Thr210) (1:200, Affinity, Catalog No: AF2385), anti-phospho-ERK1/2 (Thr202/Tyr204) (1:200, CST, Catalog No: 4370), anti-phospho-MEK (Ser221) (1:200, Affinity, Catalog No: AF3385), and anti-phospho-Akt (Ser473) (1:1000, CST, Catalog No: 4060). Next morning, the sections were rewarmed at 37 °C for 30 minutes, then incubated with the appropriate fluorescence-labeled secondary antibody (Goat anti-Rabbit IgG (H+ L) Cross-Adsorbed Secondary Antibody, Alexa Fluor 594, 1:200, Thermo Fisher Scientific Catalog No: A-11012 or Goat anti-Mouse IgG (H+ L) Cross-Adsorbed Secondary Antibody, Alexa Fluor 488, 1:200, Thermo Fisher Scientific Catalog No: A-11001) for 60 minutes after washed in PBS. The nuclei were visualized by DAPI staining, and images were obtained using a fluorescence microscope.

### Fluorescence Ubiquitination-Based Cell Cycle Indicator Reporter Cell Line Generation

The fluorescence ubiquitination-based cell cycle indicator (FUCCI) was used for live-cell imaging. The plasmid pBOB-EF1-FastFUCCI-Puro (RRID: Addgene 86849), which encodes 2 fluorescent probes (mKO2-hCDT1 and mAG-hGEM) to demarcate stages of the cell cycle, was used to construct the cell cycle reporter (FastFUCCI reporter). Following the previous protocol,<sup>24</sup> the FastFUCCI reporter was stably introduced into indicated VSMCs or control cells through lentiviral transduction. The red-, yellow-, and green-emitting populations in the FastFUCCI reporter cells corresponded to cells in G1 phase, the G1/S transition phase, and S- and/or G2-to-M phases (hereafter denoted as S/G2-M), respectively. Then, the FUCCI reporter cells were seeded in a 24-well plate at  $4 \times 10^3$  cells per well and kept in a humidified chamber under cell culture conditions for 48 hour. Images were taken using a fluorescence microscope.

### Transwell Assay

After 24 hours of the indicated treatment, the VSMCs were digested and resuspended in serum-free medium. A total of 100  $\mu$ L of cell suspension ( $5 \times 10^4$ ) was added to the upper chambers of a transwell culture plate, and 500  $\mu$ L of medium containing 10% FBS was added to the lower chambers. The plate was incubated at 37 °C and 5% CO<sub>2</sub> for 24 hour. The cells on the upper surface of the polycarbonate films were gently removed with wet cotton swabs. The polycarbonate films were carefully removed from the upper chambers, and the cells were fixed in precooled methanol for 30 minutes. The cells were then stained with 0.1%

crystal violet for 15 minutes, washed 3 times with PBS, and observed under a microscope.

### Scratch Wound Assay

VSMCs were seeded in a 6-well plate, infected, and treated. After 24 hours, a straight line was drawn across the plate with a pipette tip, and 2% FBS medium was added. Images of the scratched cells were taken after 0 and 24 hours using a microscope. The migration ability of the cells was analyzed according to the healed area of the scratch.

### Immunoprecipitation Assays

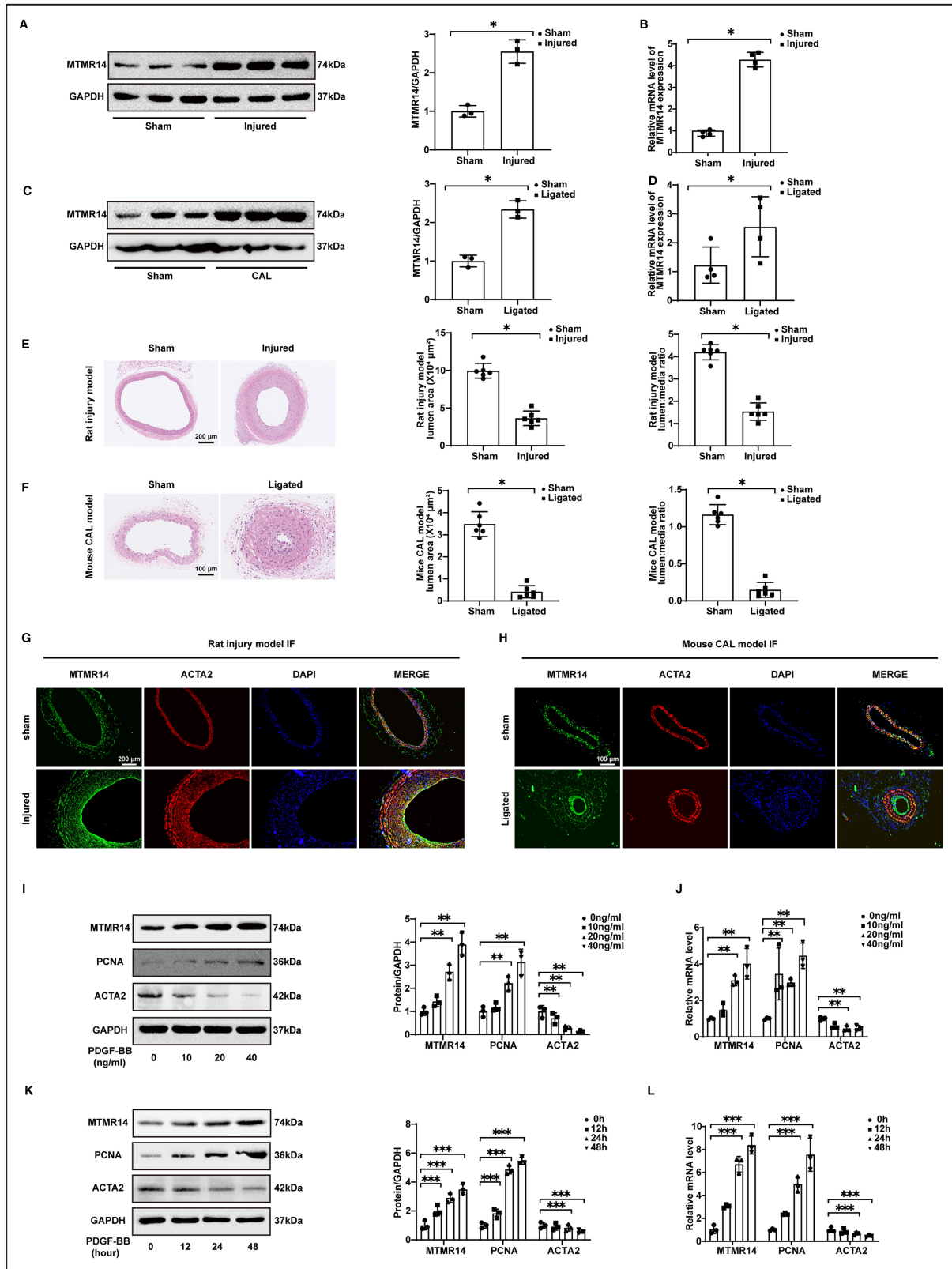
For exogenous immunoprecipitation assays, cultured 293T cells were cotransfected with the indicated plasmids for 48 hour and lysed. Supernatants were clarified by centrifugation at 13 800g for 10 minutes at 4 °C. For each immunoprecipitation, 500  $\mu$ L of the supernatant was incubated with 20  $\mu$ L of anti-Flag beads (Sigma) or anti-HA beads (Sigma) on a rotary shaker overnight at 4 °C. For endogenous immunoprecipitation, in primary VSMCs, whole-cell protein lysates were extracted, and 500  $\mu$ L of the supernatants were incubated with the corresponding antibodies as indicated and 50  $\mu$ L of protein A/G Dynabeads (Thermo Fisher Scientific) at 4 °C overnight. Finally, the beads were washed 5 to 6 times with cold immunoprecipitation buffer before adding 1 $\times$  loading buffer. Cell lysates and immunoprecipitates were eluted in loading buffer at 99 °C for 10 minutes and subjected to Western blotting.

### Silver Staining and Liquid Chromatography–Tandem Mass Spectrometry Analysis

Whole-cell protein lysates were extracted and incubated with an anti-MTMR14 antibody at 4 °C overnight. Then, the eluent was electrophoresed and silver stained the next day. Silver staining was performed using the Fast Silver Stain Kit (Beyotime Biotechnology) according to the manufacturer's instructions. Finally, the different bands were cut out and subjected to liquid chromatography–tandem mass spectrometry. Whole protein incubated with an anti-IgG antibody served as a negative control.

### Glutathione S-Transferase Pull-Down Assay

GST (glutathione S-transferase), GST-MTMR14, and GST-PLK1 were expressed and extracted from *Escherichia coli* strain BL21 (DE3) cells. Purified GST fusion proteins were immobilized on glutathione-Sepharose 4B beads (GE Healthcare, Chicago, IL) and washed with PBS. Cultured 293T cells were transfected with the indicated



plasmid (Flag-MTMR14 or Flag-PLK1) for 48hour and lysed, and then the beads were incubated with whole 293T cell extract for 6hour at 4 °C. The beads were then washed with GST binding buffer (20mM HEPES, pH 7.6,

0.1M KCl, 0.1 μM EDTA, 10% glycerol, 0.02% NP-40, and protease inhibitor cocktail), and the proteins were eluted with PBS buffer containing 10mM reduced glutathione, followed by Western blotting.

## Statistical Analysis

Data are presented as the mean±SD. Comparisons between 2 groups were performed using 2-tailed Student's *t* tests. Differences between groups were assessed using 1-way ANOVA followed by Bonferroni correction for multiple comparisons. A value of  $P<0.05$  was considered to indicate a statistically significant difference. All statistical analyses were performed using GraphPad Prism (GraphPad Prism version 6.0, La Jolla, CA).

## RESULTS

### Neointima Formation and MTMR14 Upregulated After Carotid Artery Injury in Rats and Mice

To investigate the relationship between MTMR14 and VSMC proliferation, the carotid artery balloon injury model in rats and the carotid artery ligation injury model in mice were established, and the expression of MTMR14 was determined after the injury. Compared with sham group, the expression of MTMR14 protein was significantly increased after the vascular injury procedure in the experimental subjects (Figure 1A and 1C). Quantitative real-time polymerase chain reaction was also performed and showed the same trend in mRNA expression (Figure 1B and 1D). In tissue sections, neointima formation obviously after injury both in rats and mice (Figure 1E and 1F). Immunofluorescence staining revealed that the expression of MTMR14 was significantly elevated after injury and mainly expressed in the neointima (Figure 1G and 1H). In the rat carotid artery balloon injury model, there was no ACTA2 expression in the innermost circle where MTMR14 was expressed, but most of the expression localization of MTMR14 was overlapped with that of ACTA2 (Figure 1G). In the mice carotid artery ligation model, the majority of the expression localization of MTMR14 was overlapped with that of ACTA2 (Figure 1H, although the expression of ACTA2 in neointima was dark, it was

indeed expressed). Moreover, immunohistochemistry results showed that MTMR14 was concentrated in the neointima of human restenosis artery (Figure S1A). As shown in Figure 1I and 1J, PDGF-BB stimulation dramatically upregulated MTMR14 and proliferating cell nuclear antigen (PCNA) expression and simultaneously reduced ACTA2 levels in a dose-dependent manner. Moreover, PDGF-BB (20 ng/mL) stimulation markedly upregulated MTMR14 and PCNA expression and reduced ACTA2 levels in a time-dependent manner (Figure 1K and 1L). In general, these results suggest that MTMR14 expression is positively correlated with carotid artery injury.

### MTMR14 Deficiency Facilitates Neointima Formation After Injury In Vivo

To clarify the role of MTMR14 in VSMC proliferation in vivo, a SMC-specific MTMR14-knockout (*Mtmt14Δ*) mouse model was established (Figure 2A through 2C). Western blotting was performed to verify the specific knockout of MTMR14 in *Mtmt14Δ* mice VSMCs (Figure 2D). Next, we tested the expression of other isoenzymes of MTMR phosphatase in vascular smooth muscle cells (Figure S2A). We found that MTMR11 was upregulated at the mRNA level in *Mtmt14Δ* mice VSMCs but not at the protein level (Figure S2B and S2C). Then, CAL was performed on *Mtmt14Δ* and *Mtmt14<sup>WT</sup>* mice. In tissue sections obtained 28 days after ligation, the intima of *Mtmt14Δ* and *Mtmt14<sup>WT</sup>* were thicker than their respective sham groups. The degree of thickening of *Mtmt14Δ* after ligation was more severe than that of *Mtmt14<sup>WT</sup>* (Figure 2E). These results suggest that MTMR14 deficiency contributes to neointima formation after injury.

### MTMR14 Overexpression Alleviates Neointima Formation After Injury In Vivo

Correspondingly, to assess whether MTMR14 overexpression could reduce VSMC proliferation, a SMC-specific

#### Figure 1. MTMR14 (myotubularin-related protein 14) is upregulated in proliferating vascular smooth muscle cells (VSMCs) both in vivo and in vitro.

**A and B**, Representative protein (**A**) and mRNA (**B**) levels of MTMR14 in carotid artery of rats 28 days after balloon injury (n=3); **(C and D)** Representative protein (**C**) and mRNA (**D**) levels of MTMR14 in carotid artery of mice 28 days after ligation (n=3); **(E)** Representative images of hematoxylin–eosin (HE) staining of carotid arteries in rats at 28 days after balloon injury (scale bar, 200 μm; n=6); **(F)** Representative images of HE staining of carotid arteries in mice at 28 days after ligation (scale bar, 100 μm; n=6); **(G)** Representative images of immunofluorescence staining for MTMR14 (green), ACTA2 (red) and DAPI (blue) of carotid arteries in rats at 28 days after balloon injury (scale bar, 200 μm); **(H)** Representative images of immunofluorescence staining for MTMR14 (green), ACTA2 (red), and DAPI (blue) of carotid arteries in mice at 28 days after ligation (scale bar, 100 μm); **(I and J)** Representative protein (**I**) and mRNA (**J**) levels of MTMR14, PCNA, and ACTA2 in primary VSMCs cultured at different platelet-derived growth factor BB (PDGF-BB) concentrations (n=3); **(K and L)** Representative protein (**K**) and mRNA (**L**) levels of MTMR14, PCNA, and ACTA2 in primary VSMCs cultured with PDGF-BB (20 ng/mL) at different time gradients. (\* $P<0.05$  vs sham; \*\* $P<0.05$  vs 0 ng/mL; \*\*\* $P<0.05$  vs 0 hour; n=3). ACTA2 indicates aortic alpha-actin; CAL, carotid artery ligation; IF, immunofluorescence; PCNA, proliferating cell nuclear antigen; and PDGF-BB, platelet-derived growth factor BB.

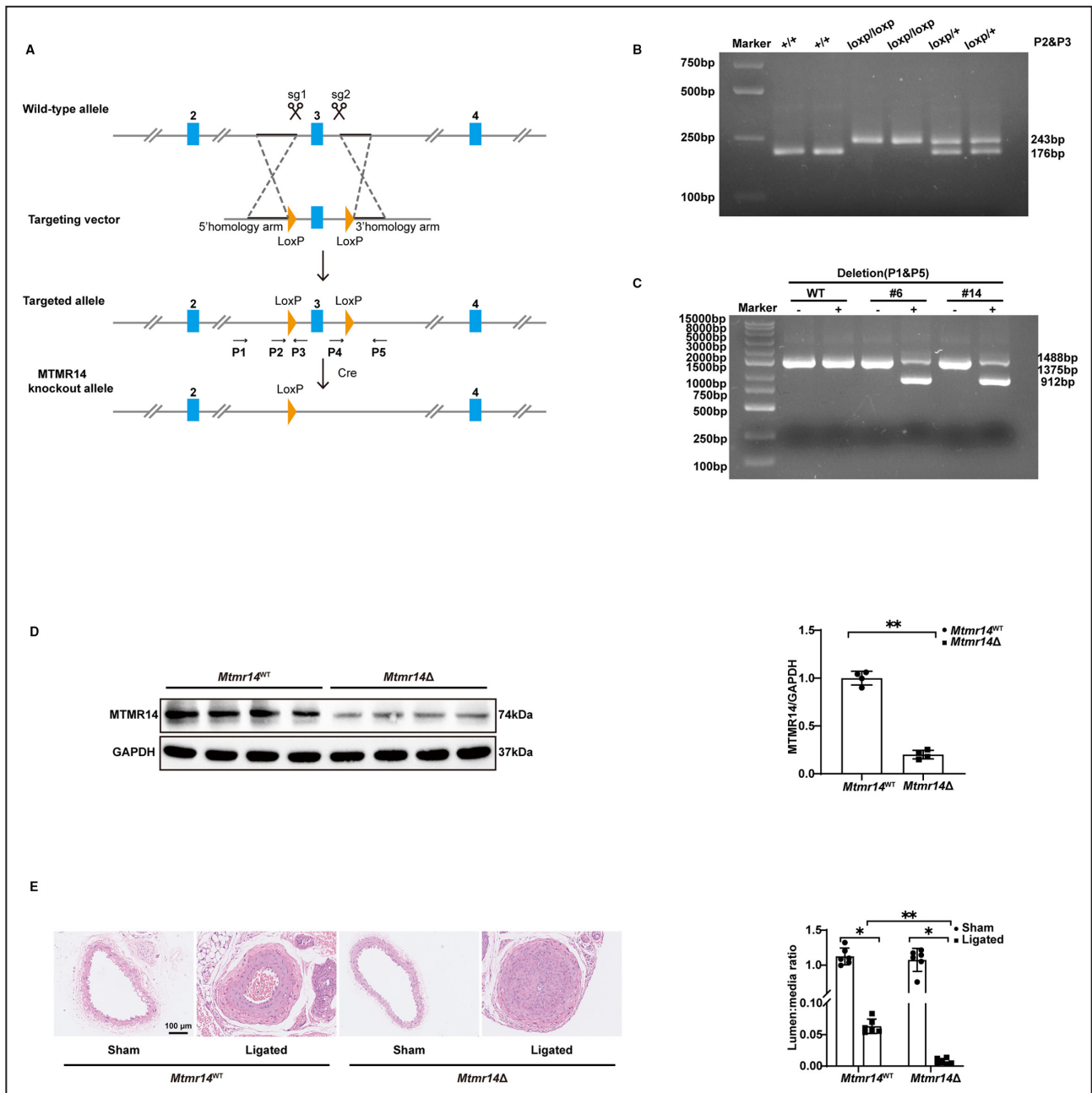


**Figure 2. MTMR14 (myotubularin-related protein 14) deficiency aggravates neointima formation.**

**A**, Schematic workflow for the construction of an SMC-specific conditional MTMR14-knockout (*Mtmr14*<sup>Δ</sup>) mouse strain; **(B)** Representative PCR amplification-mediated genotyping of MTMR14-LoxP/LoxP, MTMR14<sup>+/+</sup>, and MTMR14-LoxP/+ mice; **(C)** Mouse genotyping was confirmed by PCR; **(D)** Representative protein level of MTMR14 in carotid arteries of *Mtmr14*<sup>WT</sup> and *Mtmr14*<sup>Δ</sup> mice (n=4); **(E)** Representative hematoxylin–eosin (HE) staining images of carotid arteries in *Mtmr14*<sup>WT</sup> and *Mtmr14*<sup>Δ</sup> mice at 28 days after ligation (scale bar, 100 μm; n=6). (\**P*<0.05 vs sham, \*\**P*<0.05 vs *Mtmr14*<sup>WT</sup>). PCR indicates polymerase chain reaction; and SMC, smooth muscle cell.

MTMR14-transgenic (*Mtmr14*<sup>TG</sup>) mouse model was also established (Figure 3A). The overexpression of MTMR14 was confirmed by Western blot analyses (Figure 3B). *Mtmr14*<sup>WT</sup> and *Mtmr14*<sup>TG</sup> mice were similarly subjected to CAL as the groups described previously. Tissue sections obtained 28 days after ligation showed that the degree of neointima formation was reduced by MTMR14 overexpression with respect to sham group (Figure 3C). These

results show that MTMR14 overexpression significantly attenuates neointima formation after injury.

### MTMR14 Regulates Proliferation and Migration of VSMC In Vitro

Next, we investigated the specific role of MTMR14 in primary VSMCs. The FUCCI system was stably



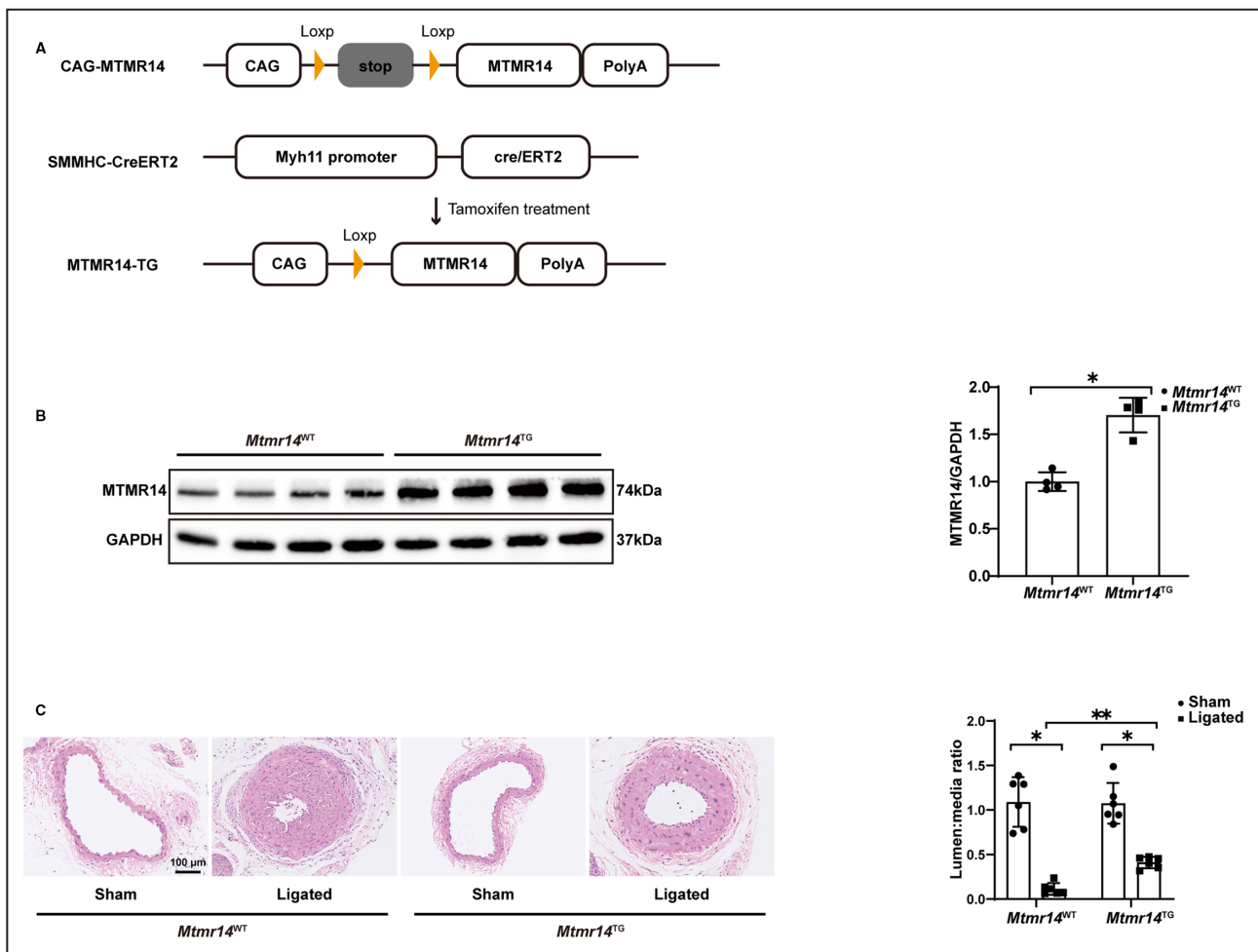


**Figure 3. Overexpression of MTMR14 (myotubularin-related protein 14) prevents neointima formation.**

**A**, Schematic workflow for the construction of a SMC-specific conditional MTMR14-transgenic (*Mtmt14<sup>TG</sup>*) mouse strain; **(B)** Representative protein level of MTMR14 in carotid arteries of *Mtmt14<sup>WT</sup>* and *Mtmt14<sup>TG</sup>* mice (n=4); **(C)** Representative hematoxylin-eosin (HE) staining images of carotid arteries in *Mtmt14<sup>WT</sup>* and *Mtmt14<sup>TG</sup>* mice at 28 days after ligation (scale bar, 100 μm; n=6). (\*P < 0.05 vs sham, \*\*P < 0.05 vs *Mtmt14<sup>WT</sup>*).

introduced into primary MTMR14-knockdown VSMCs and control cells. The cell cycle through FUCCI imaging was analyzed. After 24-hour treatment, the population of S/G2-M cells in Ad-shMTMR14 group significantly higher than that in control group (Figure 4A), suggesting that MTMR14 knockdown facilitated VSMC proliferation. In addition, transwell assays were performed to identify the effect of MTMR14 on cell migration. As shown in Figure 4B and 4C, MTMR14 knockdown significantly accelerated VSMC migration. These data reveal that MTMR14 deficiency promotes VSMC proliferation and migration.

In contrast, MTMR14 overexpression markedly reduced the number of transmembrane cells (Figure 4E), attenuated wound healing (Figure 4F), and substantially lowered the population of S/G2-M cells (Figure 4D). The results suggest that MTMR14 overexpression alleviates VSMC proliferation and migration. Collectively,

the data demonstrate that MTMR14 regulates the proliferation and migration of VSMC.

### MTMR14 Inhibits PLK1 in the Mechanism Underlying VSMC Proliferation

To thoroughly investigate the molecular mechanisms by which MTMR14 regulates VSMC proliferation, we used liquid chromatography–tandem mass spectrometry to screen the interacting proteins. The results suggested that the PLK1 was a candidate binding protein of MTMR14 (Figure 5A, Figure S3). Additionally, a series of co-immunoprecipitation experiments and GST pull-down assays confirmed that MTMR14 interacted with PLK1 both in HEK 293T cells and primary VSMCs (Figure 5B through 5G). Hence, we suspected that the PLK1 was involved in the progression of MTMR14 regulating VSMC proliferation. Interestingly, we found that the expression of MTMR14

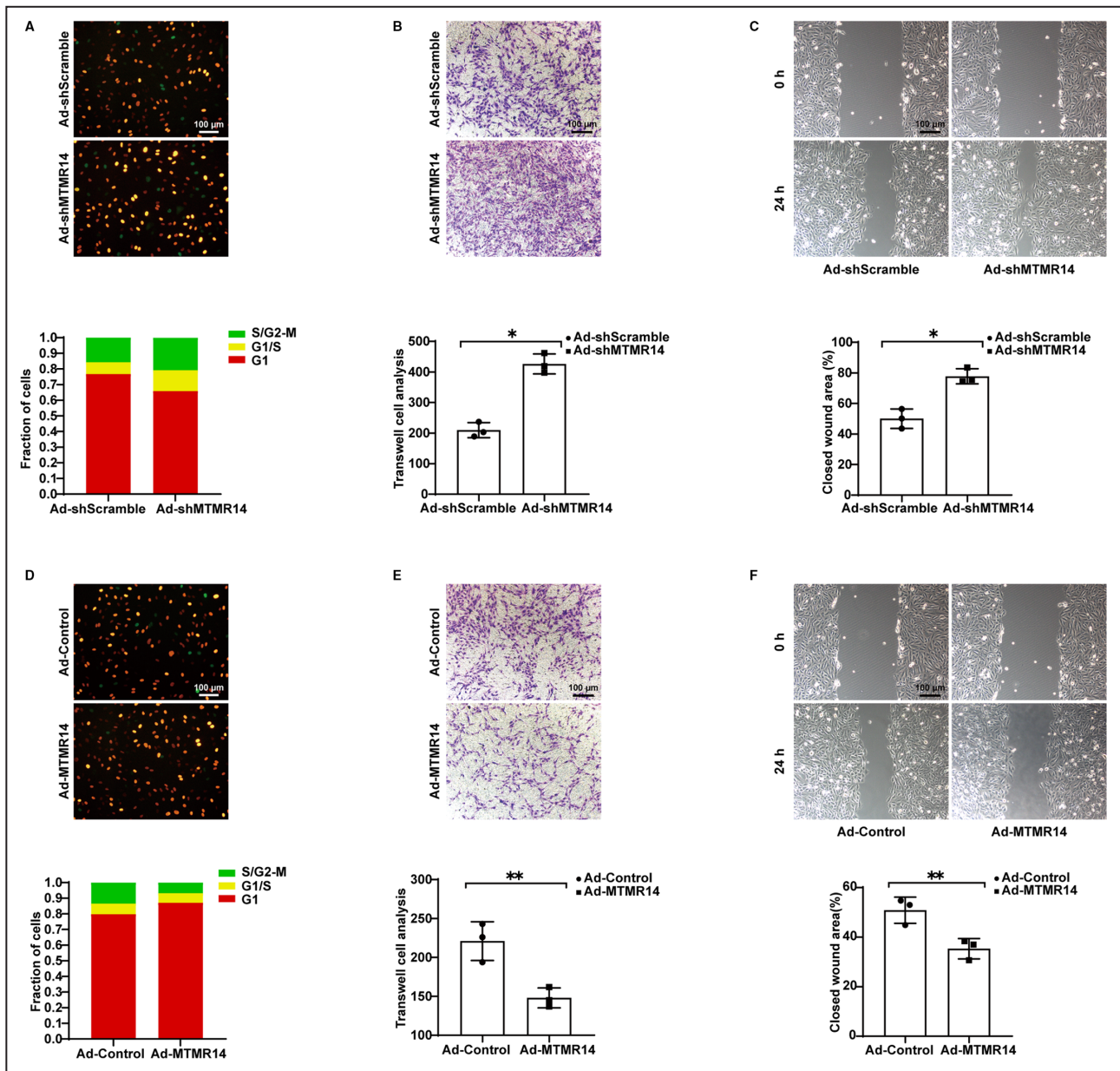


**Figure 4. The effect of MTMR14 (myotubularin-related protein 14) on proliferation and migration in primary vascular smooth muscle cells (VSMCs) stimulated by platelet-derived growth factor BB (PDGF-BB).**

**A,** Representative image of primary VSMCs stably expressing fluorescence ubiquitination-based cell cycle indicator (FUCCI) (red for G1, yellow for G1/S, green for S/G2-M) 48 hours after infection of Ad-shScramble or Ad-shMTMR14 and stimulated by 20 ng/mL PDGF-BB; **(B and C)** Transwell and scratch wound assays of primary VSMCs infected with Ad-shScramble or Ad-shMTMR14 after 20 ng/mL PDGF-BB stimulation for 24 hours; **(D)** Representative image of primary VSMCs stably expressing FUCCI cell cycle indicators (red for G1, yellow for G1/S, green for S/G2-M) 48 hours after infection of Ad-Control or Ad-MTMR14 and stimulated by 20 ng/mL PDGF-BB; **(E and F)** Transwell and scratch wound assays of primary VSMCs infected with Ad-Control or Ad-MTMR14 after 20 ng/mL PDGF-BB stimulation for 24 hours. (scale bar, 100  $\mu$ m; n=3; \* $P$ <0.05 vs Ad-shScramble, \*\* $P$ <0.05 vs Ad-Control).

increased; however, the expression of PLK1 remained unchanged in the condition of PDGF-BB intervention (Figure 5H and 5I). Moreover, what caught our attention was that the binding of MTMR14 and PLK1 was increased after PDGF-BB stimulation (Figure 5H and 5I). What's more, immunofluorescence staining

showed there was no difference in the expression of PLK1 in the neointima and media of human restenosis artery (Figure 5J).

A previous study shown that PLK1 participated in cell proliferation and migration and the cellular effects of PLK1 involved in the activation of MEK/ERK

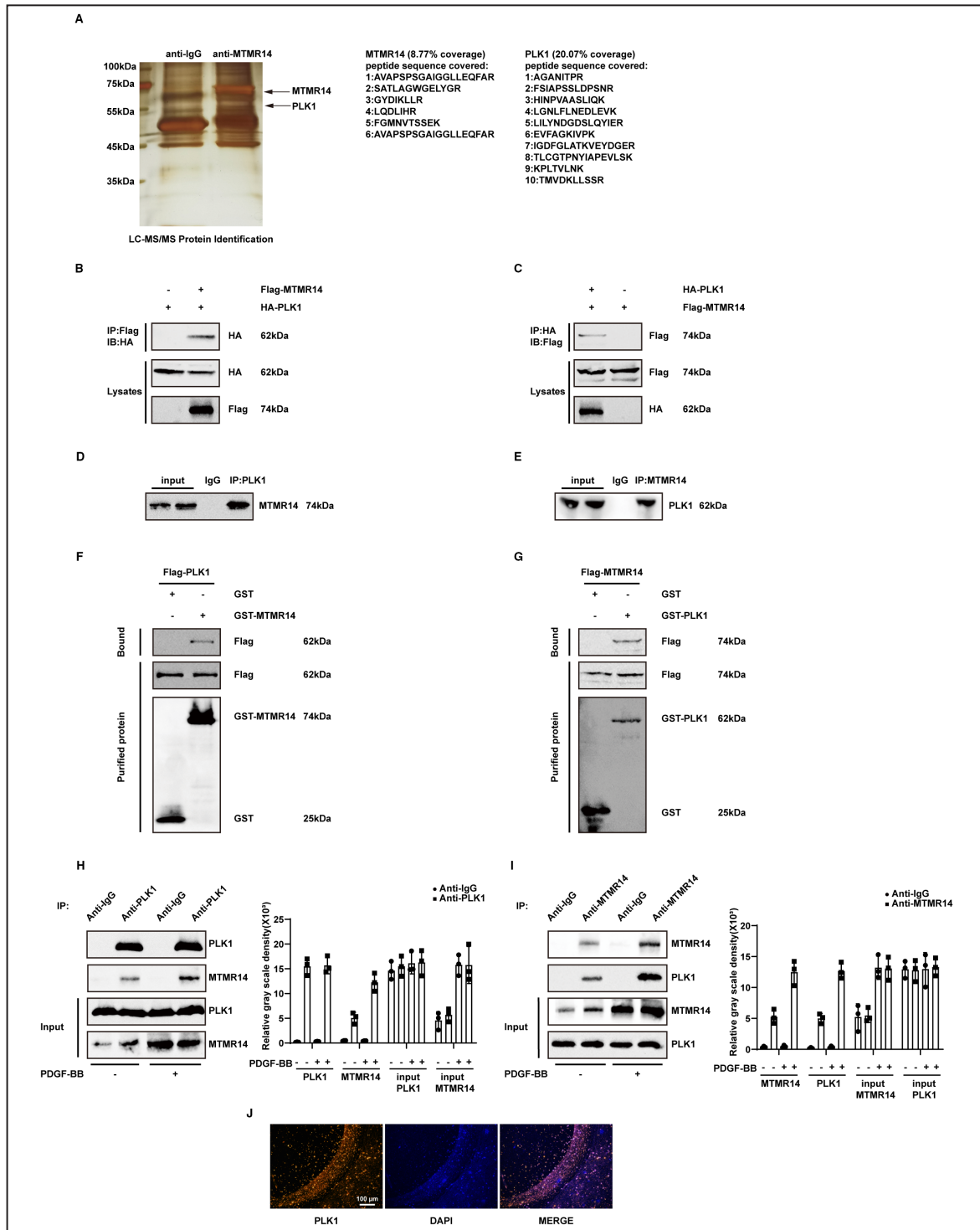
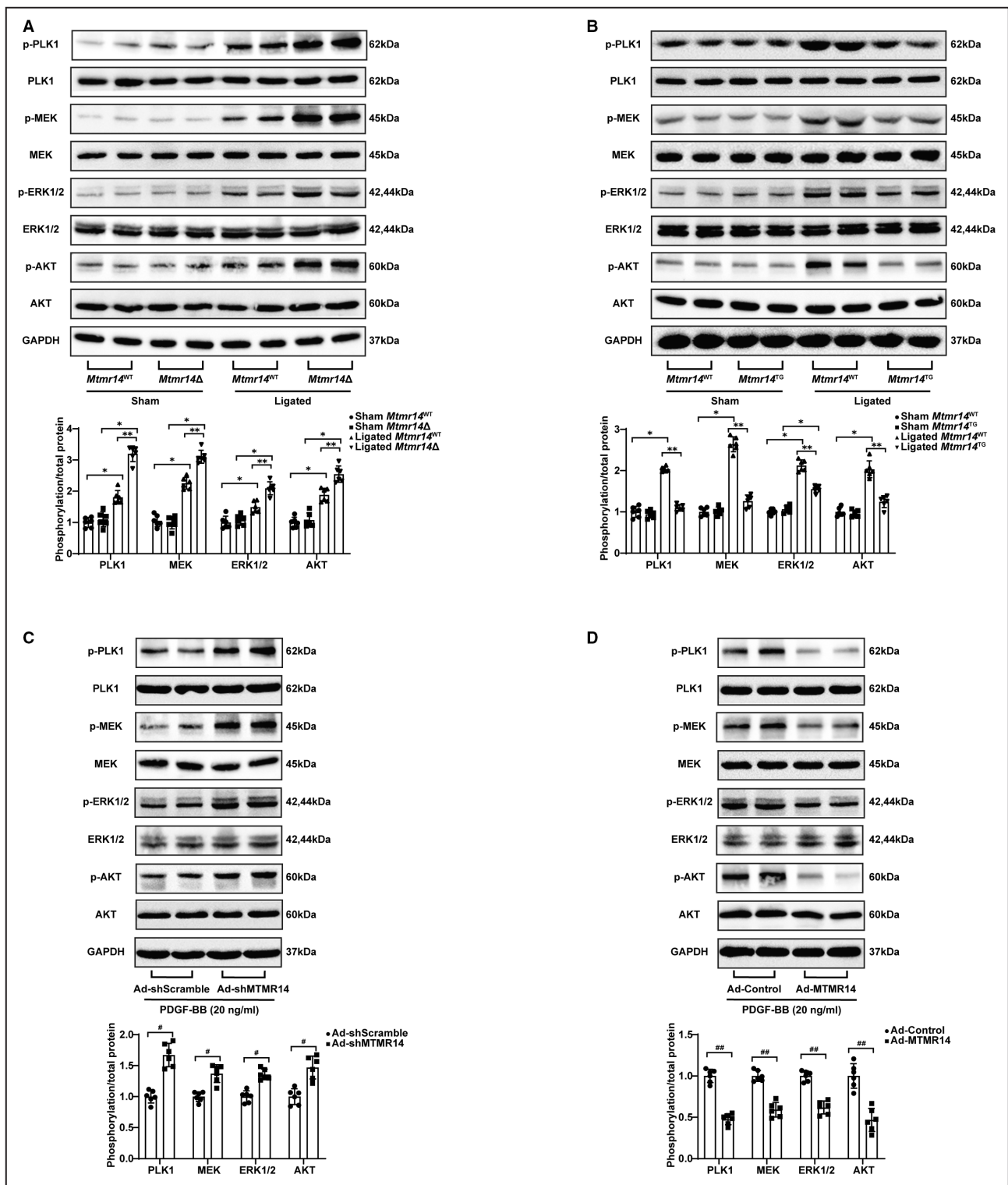


**Figure 5. MTMR14 (myotubularin-related protein 14) can bind to PLK1 (polo-like kinase 1).**

**A**, Silver-stained gel of the indicated proteins binding to MTMR14, which were coimmunoprecipitated using an anti-MTMR14 antibody and identified via mass spectrometry in primary vascular smooth muscle cells (VSMCs). IgG was used as a control; (**B** and **C**) 293T cells were transfected with plasmids expressing Flag-MTMR14 and HA-PLK1, and immunoprecipitation and Western blot assays was used to detect the binding of MTMR14 and PLK1; (**D** and **E**) immunoprecipitation and western blot assays using anti-MTMR14, and anti-PLK1 to detect the binding of MTMR14 to PLK1 in primary VSMCs. IgG was used as a control; (**F** and **G**) GST pull-down assays using anti-GST and anti-Flag to detect the direct binding of MTMR14 and PLK1. Purified GST was used as a control; (**H** and **I**) Immunoprecipitation and Western blot assays using anti-MTMR14, and anti-PLK1 to detect the binding of MTMR14 to PLK1 in primary VSMCs stimulated with or without platelet-derived growth factor BB (PDGF-BB). IgG was used as a control. **J**, Representative images of immunofluorescence staining with an anti-PLK1 antibody in slices from human restenosis artery (scale bar, 100 μm). GST, glutathione S-transferase; and LC-MS/MS, liquid chromatography–tandem mass spectrometry.



signaling pathway.<sup>25</sup> Another study also revealed that activated PLK1/ERK axis promoted cell proliferation and migration.<sup>26</sup> Then we began to focus on the role of the PLK1/MEK/ERK/AKT pathway in VSMC proliferation and migration. Further Western blotting revealed that compared with those in *Mtmr14*<sup>WT</sup> carotid VSMCs, the phosphorylation levels of PLK1, MEK, ERK1/2, and

AKT were notably upregulated in the carotid VSMCs of *Mtmr14*<sup>Δ</sup> mice after ligation (Figure 6A). However, compared with those in *Mtmr14*<sup>WT</sup> carotid VSMCs, the phosphorylation levels of PLK1, MEK, ERK1/2, and AKT were significantly attenuated in *Mtmr14*<sup>TG</sup> mice carotid VSMCs after ligation (Figure 6B). The results of in vitro experiments are consistent with those of in vivo.

Primary VSMCs were infected with Ad-shMTMR14 or Ad-MTMR14 and then treated with PDGF-BB. Phosphorylation levels of PLK1, MEK, ERK1/2, and AKT were upregulated when MTMR14 was knocked down (Figure 6C) but were downregulated when MTMR14 was overexpressed (Figure 6D). Furthermore, we detected the contraction and the proliferation marker in primary VSMCs after PDGF-BB stimulation. The results showed that manipulation of MTMR14 did not affect the expression of ATCA2 but did affect the expression of PCNA (Figure S4A and S4B). We also detected the expression of p-PLK1/p-MEK/p-ERK/p-AKT in the human restenosis section via immunofluorescence staining (Figure S4C). In summary, the results show that the activation of the PLK1/MEK/ERK1/2/AKT is suppressed by MTMR14.

### PLK1 Silencing Alleviated the MTMR14 Knockout Induced Exacerbation of Neointima Formation After Injury

To investigate whether silencing PLK1 could reverse neointima formation in *Mtmt14Δ* mice, a local infection of adenovirus was performed, and the tissue sections showed that local infection of Ad-shPLK1 alleviated the degree of neointima formation (Figure 7A). Western blotting showed that the total expression of PLK1 was reduced, confirming the success of local infection of adenovirus. The phosphorylation levels of PLK1, MEK, ERK1/2, and AKT were significantly attenuated in Ad-shPLK1 local infection *Mtmt14Δ* mice (Figure 7B), suggesting silencing PLK1 reversed the activation of PLK1/MEK/ERK/AKT pathway. Next, we observed the effect of silencing PLK1 on VSMC migration and cell cycle. Transwell assays showed that the migration of VSMC was reduced after PLK1 silencing (Figure 7D). At the same time, the quantity of cells in S/G2-M phase decreased significantly after PLK1 silencing (Figure 7E). The detection of the contraction and the proliferation markers showed that the expression of PCNA was upregulated in *Mtmt14Δ* mice; however, the expression of PCNA was restored after PLK1 silencing. The expression of ACTA2 was not affected by PLK1 silencing in *Mtmt14Δ* mice (Figure 7C). These results indicate

that neointima formation and VSMC proliferation and migration are inhibited when the activation of PLK1 is blocked.

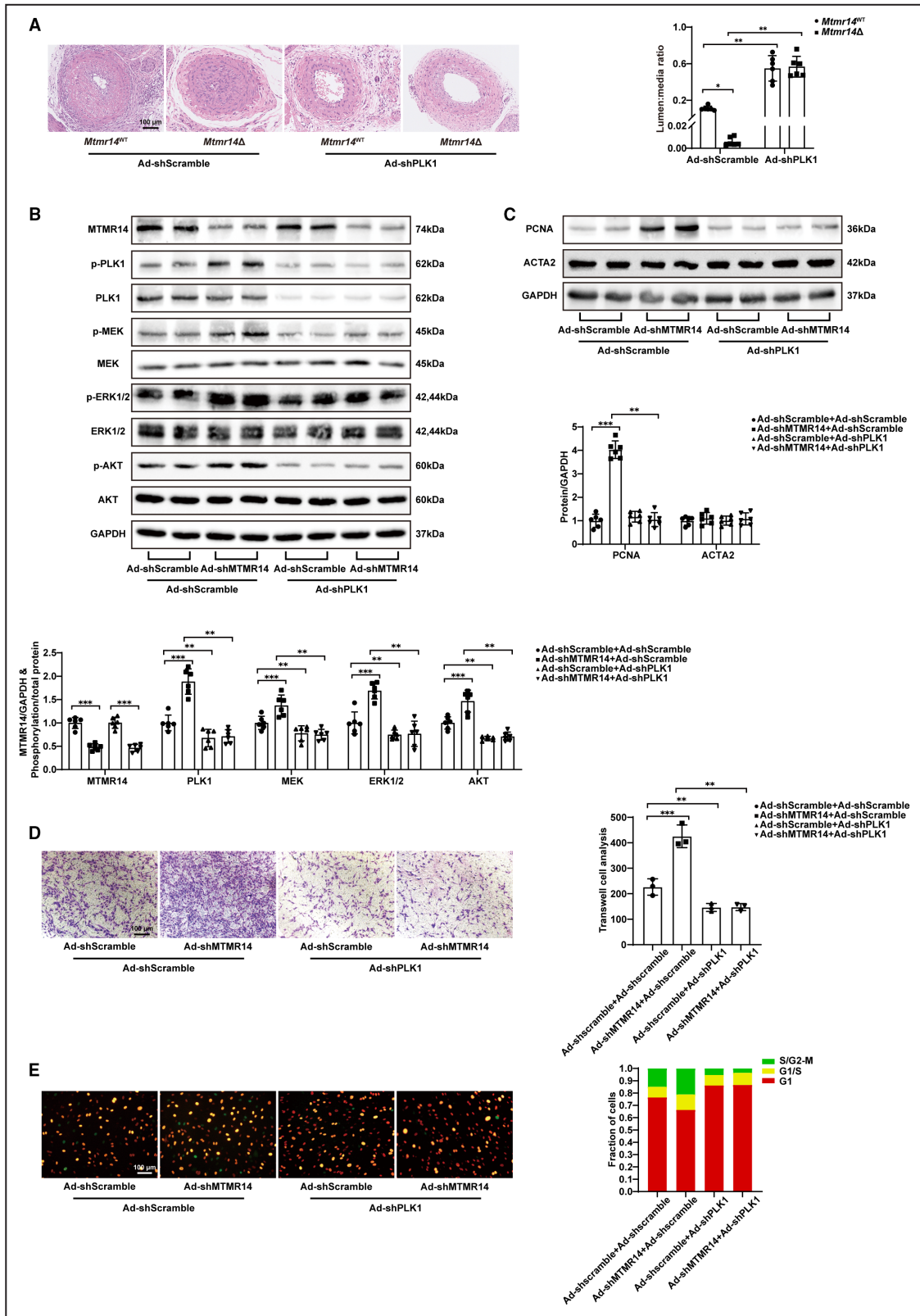
Next, we investigated whether overexpression of PLK1 antagonizes the inhibitory effect of MTMR14 overexpression on neointima formation after injury. In *Mtmt14<sup>TG</sup>* mice, a local infection of adenovirus was performed, and the tissue sections showed that local infection of Ad-PLK1 offset the inhibitory effect of MTMR14 overexpression on neointima formation. Besides, local infection of Ad-PLK1 in *Mtmt14<sup>TG</sup>* mice significantly exacerbated the degree of neointima formation (Figure S5A). Western blotting showed that the phosphorylation levels of PLK1, MEK, ERK1/2, and AKT were significantly upregulated in Ad-PLK1 local infection *Mtmt14<sup>TG</sup>* mice (Figure S5B), suggesting overexpression PLK1 promoted the activation of PLK1/MEK/ERK/AKT pathway. As for the contraction and the proliferation markers, the detection results showed that the expression of PCNA was reduced in *Mtmt14<sup>TG</sup>* mice, but the expression of PCNA was increased after the local infection of Ad-PLK1. However, the expression of ACTA2 was not affected by PLK1 overexpression in *Mtmt14<sup>TG</sup>* mice (Figure S5C). The results suggest that excessive activation of PLK1 promotes neointima formation and VSMC proliferation and migration.

## DISCUSSION

VSMCs are highly differentiated and specialized cells that constitute the main component of the vessel wall, but they are not terminally differentiated cells. Vascular injuries such as percutaneous transluminal angioplasty, cutting balloon angioplasty, rotational atherectomy, and stenting can lead to complex changes in VSMC behavior, function, antioxidant status, and inflammatory response,<sup>27–29</sup> which contribute to the proliferation of VSMC from the media to the intima and increase synthesis of collagen, elastin, and a proteoglycan matrix and lead to neointima formation eventually.<sup>30</sup> VSMC proliferation is an elementary step and plays a crucial role in restenosis.<sup>30–32</sup> However, the exact mechanism underlying VSMC proliferation remains poorly understood.

### Figure 6. The impact of MTMR14 (myotubularin-related protein 14) on PLK1 (polo-like kinase 1) is mediated by inhibiting the phosphorylation of PLK1.

**A**, Western blot assays were performed in the carotid arteries tissues in *Mtmt14<sup>WT</sup>* or MTMR14-knockout (*Mtmt14Δ*) mice at 28 days after ligation to detect the expression of PLK1, p-PLK1, MEK, p-MEK, ERK1/2, p-ERK1/2, AKT, and p-AKT; **(B)** Western blot assays were performed in the carotid arteries in *Mtmt14<sup>WT</sup>* or MTMR14-transgenic (*Mtmt14<sup>TG</sup>*) mice at 28 days after ligation to detect the expression of PLK1, p-PLK1, MEK, p-MEK, ERK1/2, p-ERK1/2, AKT, and p-AKT; **(C)** Western blot assays were performed in primary vascular smooth muscle cells (VSMCs) infected with Ad-shScramble or Ad-shMTMR14 at 24 hours after platelet-derived growth factor BB (PDGF-BB) stimulation to detect the expression of PLK1, p-PLK1, MEK, p-MEK, ERK1/2, p-ERK1/2, AKT, and p-AKT; **(D)** Western blot assays were performed in primary VSMCs infected with Ad-Control or Ad-MTMR14 at 24 hours after PDGF-BB stimulation to detect the expression of PLK1, p-PLK1, MEK, p-MEK, ERK1/2, p-ERK1/2, AKT, and p-AKT. (GAPDH served as the loading control, n=6, \*P<0.05 vs sham, \*\*P<0.05 vs *Mtmt14<sup>WT</sup>* #P<0.05 vs Ad-shScramble, ##P<0.05 vs Ad-Control). AKT indicates protein kinase B; ERK, extracellular-signal-regulated kinase; and MEK, mitogen-activated protein kinase kinase.



MTMR14, a novel phosphoinositide phosphatase conserved through evolution, specifically dephosphorylates phosphatidylinositol 3,5-bisphosphate (PtdIns(3,5)P<sub>2</sub>) and phosphatidylinositol 3-phosphate (PtdIns3P). The

molecule is involved in a variety of biological processes. It was first identified as a specific phosphatase of skeletal muscle and studied in centronuclear myopathy,<sup>33,34</sup> and the deficiency of MTMR14 contributes to the accumulation

**Figure 7. Knockdown PLK1 (polo-like kinase 1) reversed the neointima formation aggravated by MTMR14 (myotubularin-related protein 14) knockdown.**

**A**, Representative hematoxylin–eosin (HE) staining images of carotid arteries from *Mttr14*<sup>WT</sup> or MTMR14-knockout (*Mttr14* $\Delta$ ) mice local infected with Ad-shScramble or Ad-shPLK1 at 28 days after ligation (scale bar, 100  $\mu$ m; n=6); **(B)** Western blot assays were performed in primary vascular smooth muscle cells (VSMCs) infected with Ad-shScramble+Ad-shScramble, Ad-shMTMR14+ Ad-shScramble, Ad-shScramble+Ad-PLK1, or Ad-shMTMR14+ Ad-shPLK1 at 24 hours after 20 ng/mL platelet-derived growth factor BB (PDGF-BB) stimulation to detect the expression of PLK1, p-PLK1, MEK, p-MEK, ERK1/2, p-ERK1/2, AKT, and p-AKT (GAPDH served as the loading control, n=6); **(C)** Western blot assays were performed in primary VSMCs infected with Ad-shScramble+ Ad-shScramble, Ad-shMTMR14+ Ad-shScramble, Ad-shMTMR14+ Ad-shPLK1 or Ad-shMTMR14+ Ad-shPLK1 after 20 ng/mL PDGF-BB stimulation for 24 hours to detect the expression of PCNA and ACTA2 (GAPDH served as the loading control, n=6); **(D)** Transwell assays of primary VSMCs infected with Ad-shScramble+ Ad-shScramble, Ad-shMTMR14+ Ad-shScramble, Ad-shMTMR14+ Ad-shPLK1 or Ad-shMTMR14+ Ad-shPLK1 after 20 ng/mL PDGF-BB stimulation for 24 hours (scale bar, 100  $\mu$ m; n=3); **(E)** Representative image of primary VSMCs stably expressing fluorescence ubiquitination-based cell cycle indicator (FUCCI) (red for G1, yellow for G1/S, green for S/G2-M) 48 hours after infection of Ad-shScramble+ Ad-shScramble, Ad-shMTMR14+ Ad-shScramble, Ad-shMTMR14+ Ad-shPLK1 or Ad-shMTMR14+ Ad-shPLK1 and stimulated by 20 ng/mL PDGF-BB (scale bar, 100  $\mu$ m). (\* $P$ <0.05 *Mttr14* $\Delta$  vs *Mttr14*<sup>WT</sup>, \*\* $P$ <0.05 Ad-shPLK1 vs Ad-shScramble, \*\*\* $P$ <0.05 Ad-shMTMR14 vs Ad-shScramble). ACTA2 indicates aortic alpha-actin; AKT, protein kinase B; ERK, extracellular-signal-regulated kinase; MEK, mitogen-activated protein kinase kinase; and PCNA, proliferating cell nuclear antigen.

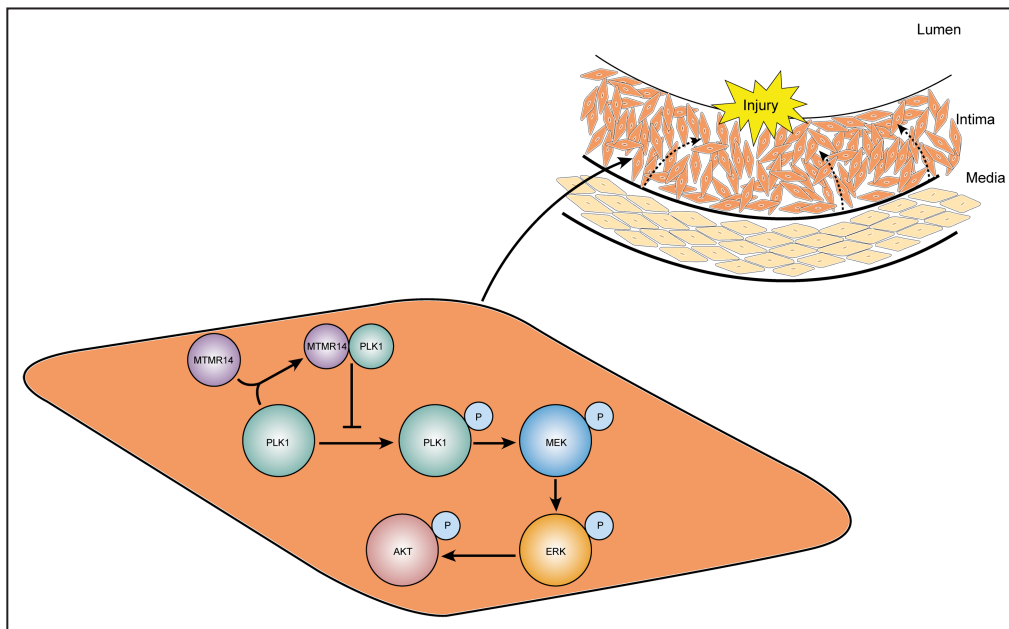


**Figure 8. MTMR14 (myotubularin-related protein 14) prevents neointima formation and vascular smooth muscle cell proliferation by inhibiting PLK1/MEK/ERK/AKT axis.**

PLK1/MEK/ERK/AKT axis was activated in vascular smooth muscle cells (VSMCs) after injury promoting VSMC proliferation and neointima formation. MTMR14 inhibited the activation of PLK1 (polo-like kinase 1) by interacting with PLK1, which further inhibited the activation of the MEK/ERK/AKT axis, thereby inhibiting VSMC proliferation and neointima formation. ACTA2 indicates aortic alpha-actin; AKT, protein kinase B; CAL, carotid artery ligation; ERK, extracellular-signal-regulated kinase; FUCCI, fluorescence ubiquitination-based cell cycle indicator; HE, hematoxylin–eosin; MEK, mitogen-activated protein kinase kinase; PCNA, proliferating cell nuclear antigen; and PDGF-BB, platelet-derived growth factor BB.

of PtdIns(3,5)P<sub>2</sub> within the muscle sarcoplasmic reticulum, leading to Ca<sup>2+</sup> homeostasis defects and causing muscle function disorder.<sup>35</sup> Further study indicated that MTMR14 inactivation leads to a series of late-onset inflammation and metabolic dysfunction, which may be regulated by the PI3K/Akt and ERK signaling pathways.<sup>36,37</sup> Similarly, our recent study revealed that MTMR14 overexpression alleviates pressure overload-induced cardiac hypertrophy by inhibiting Akt.<sup>12</sup> In addition, research has shown that MTMR14 plays a vital role in regulating mouse embryonic

fibroblast proliferation; more specifically, the growth factor induced PI3K/AKT and MEK/ERK signaling pathways may underlie this process.<sup>10</sup> These previous studies indicated that MTMR14 may be related to cell proliferation, whereas the study of MTMR14 in VSMC proliferation has not been reported.

In the present research, we found that the expression of MTMR14 was upregulated and neointimal formation in injured carotid artery. Then, we carried out a series of experiments to investigate the role of

MTMR14 in neointimal formation and VSMC proliferation after vessel injury. The VSMC contractile marker, ACTA2, was downregulated, and the VSMC proliferation marker, PCNA, was simultaneously upregulated, which indicating VSMC dedifferentiated into a synthetic proliferative state. By knocking out MTMR14, neointimal formation was aggravated and the proliferation of VSMC were promoted. Moreover, we got opposite results when MTMR14 was overexpressed both in vivo and in vitro. These results indicated that MTMR14 plays a key role in neointima formation and VSMC proliferation. To further explore the mechanism of MTMR14 in neointima formation and VSMC proliferation, liquid chromatography–tandem mass spectrometry was used to screen the interacting proteins. The results suggested that MTMR14 may function by binding to PLK1. Interestingly, under the condition of PDGF-BB intervention, the MTMR14 expression was increased but the PLK1 expression remained unchanged, and immunoprecipitation assay showed the binding of MTMR14 and PLK1 was increased after PDGF-BB stimulation. We considered that it might be the increasing binding of MTMR14 and PLK1 after PDGF-BB stimulation, and the increased binding might be caused by the increased expression of MTMR14. Additionally, immunofluorescence staining showed there was no difference in the expression of PLK1 in the neointima and media of human restenosis artery, suggesting that activated PLK1 may be involved in this process rather than total PLK1.

Interestingly, we noticed that some parts seem to lack the colocalization of ACTA2 and MTMR14 in the immunofluorescence staining experiments of rat artery injury model and mouse CAL model. After carefully analyzed, in rat artery injury model, most of the expression localization of MTMR14 was overlapped with that of ACTA2; however, some parts of ACTA2 and MTMR14 were not colocalized in the innermost layer. In mouse CAL model, ACTA2 and MTMR14 were indeed colocalized, but the fluorescence of MTMR14 masks that of ACTA2 in MERGE. (We individually zoomed in the immunofluorescence-stained portion of the inner layer of ACTA2 in the mouse CAL model to show that although the innermost layer of ACTA2 is dimly fluorescent, it is indeed expressed, the data are presented in Figure S1B). As for the part of cells lacking the colocalization of ACTA2 and MTMR14, we speculated that they might be other cells involved in this pathological process, such as macrophages or intimal VSMCs lacked detectable expression of ACTA2. First, macrophages participate and play a very critical role in the formation of atherosclerosis<sup>38–40</sup>; moreover, the activation of inflammatory pathways in lesional macrophages is a critical proatherogenic process.<sup>41,42</sup> In the carotid artery injury model, the process of tissue repair was accompanied by a certain degree of inflammatory response, during which macrophages might participate and stay in

the neointima. Second, studies have shown that in some atherosclerotic lesions, there are intimal VSMCs that lack detectable ACTA2, myh11, and SM22a/Tagln, which are the markers traditionally used to identify VSMCs.<sup>43,44</sup> In addition, under some conditions VSMCs downregulate VSMC markers and express macrophage markers such as CD68 and Mac2.<sup>45</sup> As to what those cells lacking in colocalization of ACTA2 and MTMR14 are, we will conduct further investigations.

PLK1, a prototypical member of the PLK family, is a serine/threonine protein kinase widely found in many eukaryotic cells. PLK1 plays an essential role in initiation, maintenance, and completion of mitosis. The expression of PLK1 is upregulated in actively proliferating cells and varies substantially at different stages of the cell cycle.<sup>46</sup> PLK1 participates in regulating abscission in mitosis through interacting with the MTMR protein family members<sup>47</sup> and is required for vascular homeostasis and participates in VSMC proliferation.<sup>48–50</sup> Previous studies demonstrated that PLK1 participate in regulating cell proliferation through activating MEK/ERK(MAPK; mitogen-activated protein kinase) signaling pathway.<sup>25,26,51</sup> MAPK signaling pathway acts as an integration point for multiple biochemical signals and is involved in a variety of cellular processes such as proliferation, differentiation, transcription regulation, and development.<sup>52,53</sup> Many studies indicated that MAPK promotes neointima formation.<sup>54–57</sup> In the present study, we demonstrated that MTMR14 inhibited the activation of PLK1 by interacting with PLK1 and further inhibited the activation of the MEK/ERK/AKT axis, thereby inhibiting VSMC proliferation and neointima formation (Figure 8).

As a serine/threonine kinase, AKT plays a vital role in cardiac hypertrophy, which has been widely studied.<sup>58–61</sup> Previous study carried out by our team showed that MTMR14 suppresses cardiac hypertrophy by inhibiting AKT.<sup>12</sup> Moreover, inhibition of PLK1 suppressed downstream signaling AKT.<sup>62</sup> Interestingly, in this study, we found that p-AKT is decreased when MTMR14 is overexpressed or PLK1 is silenced in VSMCs, similar to the results in cardiac hypertrophy. We hypothesized that MTMR14 may inhibit p-AKT by interacting with PLK1 in VSMCs. However, the specific mechanism of p-AKT inhibition by MTMR14 has not been clarified in this study or our previous study on cardiac hypertrophy, which is worthy of further investigation.

## CONCLUSIONS

In the present study, we found that MTMR14 overexpression suppresses VSMC proliferation by inhibiting PLK1, which provides a new avenue for further investigating VSMC proliferation. However, whether MTMR14 dephosphorylates PLK1 directly or is mediated by phosphoinositides as second messengers remains unclear. A thorough exploration of the potential



molecular mechanism between MTMR14 and PLK1 in VSMC proliferation may provide therapeutic guidance in the treatment of restenosis.

## ARTICLE INFORMATION

Received March 18, 2022; accepted August 17, 2022.

### Affiliations

Department of Cardiology, The First Affiliated Hospital of Zhengzhou University, Zhengzhou University, Zhengzhou, China (L.K., C.L., P.L., D.Z., R.Y., L.Y., Z.H., X.T., C.G., B.D., J.D., Y.Z.); The Second School of Clinical Medicine, Southern Medical University, Guangzhou, China (Y.Z.); Department of Cardiology, The 7th People's Hospital of Zhengzhou, Zhengzhou, China (S.F.); Department of Thoracic Surgery (H.Z.); and Department of Cardiovascular Surgery (H.Z.), Union Hospital, Wuhan, China; and Department of Cardiology, Beijing Anzhen Hospital, Capital Medical University, National Clinical Research Centre for Cardiovascular Diseases, Beijing, China (J.D.).

### Sources of Funding

This work was supported by grants from the National Natural Science Foundation of China (81770048 and 81970242); and Henan Province Health Planning Technology Talents Overseas Research Project (formerly 5451 Project, HWYX2019045).

### Disclosures

None.

### Supplemental Material

Table S1  
Figure S1–S5

## REFERENCES

- DALYs GBD and Collaborators H. Global, regional, and national disability-adjusted life-years (DALYs) for 333 diseases and injuries and healthy life expectancy (HALE) for 195 countries and territories, 1990–2016: a systematic analysis for the Global Burden of Disease Study 2016. *Lancet*. 2017;390:1260–1344. doi: [10.1016/S0140-6736\(17\)32130-X](https://doi.org/10.1016/S0140-6736(17)32130-X)
- Collaborators GBDCoD. Global, regional, and national age-sex specific mortality for 264 causes of death, 1980–2016: a systematic analysis for the Global Burden of Disease Study 2016. *Lancet*. 2017;390:1151–1210. doi: [10.1016/S0140-6736\(17\)32152-9](https://doi.org/10.1016/S0140-6736(17)32152-9)
- Durham AL, Speer MY, Scatena M, Giachelli CM, Shanahan CM. Role of smooth muscle cells in vascular calcification: implications in atherosclerosis and arterial stiffness. *Cardiovasc Res*. 2018;114:590–600. doi: [10.1093/cvr/cvy010](https://doi.org/10.1093/cvr/cvy010)
- Bennett MR, Sinha S, Owens GK. Vascular smooth muscle cells in atherosclerosis. *Circ Res*. 2016;118:692–702. doi: [10.1161/CIRCRESAHA.115.306361](https://doi.org/10.1161/CIRCRESAHA.115.306361)
- Grootaert MOJ, Moulis M, Roth L, Martinet W, Vindis C, Bennett MR, De Meyer GRY. Vascular smooth muscle cell death, autophagy and senescence in atherosclerosis. *Cardiovasc Res*. 2018;114:622–634. doi: [10.1093/cvr/cvy007](https://doi.org/10.1093/cvr/cvy007)
- Chistiakov DA, Orekhov AN, Bobryshev YV. Vascular smooth muscle cell in atherosclerosis. *Acta Physiol (Oxf)*. 2015;214:33–50. doi: [10.1111/apha.12466](https://doi.org/10.1111/apha.12466)
- Robinson FL, Dixon JE. Myotubularin phosphatases: policing 3-phosphoinositides. *Trends Cell Biol*. 2006;16:403–412. doi: [10.1016/j.tcb.2006.06.001](https://doi.org/10.1016/j.tcb.2006.06.001)
- Manzeger A, Tagscherer K, Lorincz P, Szaker H, Lukacsovich T, Pilz P, Kmezcik R, Csikos G, Erdelyi M, Sass M, et al. Condition-dependent functional shift of two Drosophila MTMR lipid phosphatases in autophagy control. *Autophagy*. 2021;1–19:4010–4028. doi: [10.1080/15548627.2021.1899681](https://doi.org/10.1080/15548627.2021.1899681)
- Hnia K, Vaccari I, Bolino A, Laporte J. Myotubularin phosphoinositide phosphatases: cellular functions and disease pathophysiology. *Trends Mol Med*. 2012;18:317–327. doi: [10.1016/j.molmed.2012.04.004](https://doi.org/10.1016/j.molmed.2012.04.004)
- Liu J, Lv Y, Liu QH, Qu CK, Shen J. Deficiency of MTMR14 promotes autophagy and proliferation of mouse embryonic fibroblasts. *Mol Cell Biochem*. 2014;392:31–37. doi: [10.1007/s11010-014-2015-5](https://doi.org/10.1007/s11010-014-2015-5)
- Li S, Zhang M, Zhang B. MTMR14 protects against hepatic ischemia-reperfusion injury through interacting with AKT signaling in vivo and in vitro. *Biomed Pharmacother*. 2020;129:110455. doi: [10.1016/j.biopha.2020.110455](https://doi.org/10.1016/j.biopha.2020.110455)
- Zhang JL, Zhang DH, Li YP, Wu LM, Liang C, Yao R, Wang Z, Feng SD, Wang ZM, Zhang YZ. Myotubularin-related protein 14 suppresses cardiac hypertrophy by inhibiting Akt. *Cell Death Dis*. 2020;11:140. doi: [10.1038/s41419-020-2330-6](https://doi.org/10.1038/s41419-020-2330-6)
- Holtrich U, Wolf G, Brauning A, Karn T, Bohme B, Rubsam-Waigmann H, Strebhardt K. Induction and down-regulation of PLK, a human serine/threonine kinase expressed in proliferating cells and tumors. *Proc Natl Acad Sci USA*. 1994;91:1736–1740. doi: [10.1073/pnas.91.5.1736](https://doi.org/10.1073/pnas.91.5.1736)
- van de Weerd BC, Medema RH. Polo-like kinases: a team in control of the division. *Cell Cycle*. 2006;5:853–864. doi: [10.4161/cc.5.8.2692](https://doi.org/10.4161/cc.5.8.2692)
- Takaki T, Trenz K, Costanzo V, Petronczki M. Polo-like kinase 1 reaches beyond mitosis—cytokinesis, DNA damage response, and development. *Curr Opin Cell Biol*. 2008;20:650–660. doi: [10.1016/j.ccb.2008.10.005](https://doi.org/10.1016/j.ccb.2008.10.005)
- Strebhardt K. Multifaceted polo-like kinases: drug targets and anti-targets for cancer therapy. *Nat Rev Drug Discov*. 2010;9:643–660. doi: [10.1038/nrd3184](https://doi.org/10.1038/nrd3184)
- Petronczki M, Lenart P, Peters JM. Polo on the rise—from mitotic entry to cytokinesis with Plk1. *Dev Cell*. 2008;14:646–659. doi: [10.1016/j.devcel.2008.04.014](https://doi.org/10.1016/j.devcel.2008.04.014)
- Glover DM, Hagan IM, Tavares AA. Polo-like kinases: a team that plays throughout mitosis. *Genes Dev*. 1998;12:3777–3787. doi: [10.1101/gad.12.24.3777](https://doi.org/10.1101/gad.12.24.3777)
- Barr FA, Sillje HH, Nigg EA. Polo-like kinases and the orchestration of cell division. *Nat Rev Mol Cell Biol*. 2004;5:429–440. doi: [10.1038/nrm1401](https://doi.org/10.1038/nrm1401)
- Barr FA, Gruneberg U. Cytokinesis: placing and making the final cut. *Cell*. 2007;131:847–860. doi: [10.1016/j.cell.2007.11.011](https://doi.org/10.1016/j.cell.2007.11.011)
- Archambault V, Glover DM. Polo-like kinases: conservation and divergence in their functions and regulation. *Nat Rev Mol Cell Biol*. 2009;10:265–275. doi: [10.1038/nrm2653](https://doi.org/10.1038/nrm2653)
- Sur S, Swier VJ, Radwan MM, Agrawal DK. Increased expression of phosphorylated polo-like kinase 1 and histone in bypass vein graft and coronary arteries following angioplasty. *PLoS One*. 2016;11:e0147937. doi: [10.1371/journal.pone.0147937](https://doi.org/10.1371/journal.pone.0147937)
- Satoh K, Matoba T, Suzuki J, O'Dell MR, Nigro P, Cui Z, Mohan A, Pan S, Li L, Jin ZG, et al. Cyclophilin A mediates vascular remodeling by promoting inflammation and vascular smooth muscle cell proliferation. *Circulation*. 2008;117:3088–3098. doi: [10.1161/CIRCULATIONAHA.107.756106](https://doi.org/10.1161/CIRCULATIONAHA.107.756106)
- Koh SB, Mascalchi P, Rodriguez E, Lin Y, Jodrell DI, Richards FM, Lyons SK. A quantitative FastFUCCL assay defines cell cycle dynamics at a single-cell level. *J Cell Sci*. 2017;130:512–520. doi: [10.1242/jcs.195164](https://doi.org/10.1242/jcs.195164)
- Wu J, Ivanov AI, Fisher PB, Fu Z. Polo-like kinase 1 induces epithelial-to-mesenchymal transition and promotes epithelial cell motility by activating CRAF/ERK signaling. *Elife*. 2016;5. doi: [10.7554/eLife.10734](https://doi.org/10.7554/eLife.10734)
- Zhang C, Wang X, Fang D, Xu P, Mo X, Hu C, Abdelatty A, Wang M, Xu H, Sun Q, et al. STK39 is a novel kinase contributing to the progression of hepatocellular carcinoma by the PLK1/ERK signaling pathway. *Theranostics*. 2021;11:2108–2122. doi: [10.7150/thno.48112](https://doi.org/10.7150/thno.48112)
- Aizik G, Grad E, Golomb G. Monocyte-mediated drug delivery systems for the treatment of cardiovascular diseases. *Drug Deliv Transl Res*. 2018;8:868–882. doi: [10.1007/s13346-017-0431-2](https://doi.org/10.1007/s13346-017-0431-2)
- Owens GK, Kumar MS, Wamhoff BR. Molecular regulation of vascular smooth muscle cell differentiation in development and disease. *Physiol Rev*. 2004;84:767–801. doi: [10.1152/physrev.00041.2003](https://doi.org/10.1152/physrev.00041.2003)
- Gomez D, Owens GK. Smooth muscle cell phenotypic switching in atherosclerosis. *Cardiovasc Res*. 2012;95:156–164. doi: [10.1093/cvr/cvs115](https://doi.org/10.1093/cvr/cvs115)
- Lange RA, Flores ED, Hillis LD. Restenosis after coronary balloon angioplasty. *Annu Rev Med*. 1991;42:127–132. doi: [10.1146/annurev.med.42.020191.001015](https://doi.org/10.1146/annurev.med.42.020191.001015)
- Chen LJ, Lim SH, Yeh YT, Lien SC, Chiu JJ. Roles of microRNAs in atherosclerosis and restenosis. *J Biomed Sci*. 2012;19:79. doi: [10.1186/1423-0127-19-79](https://doi.org/10.1186/1423-0127-19-79)
- Indolfi C, Cioppa A, Stabile E, Di Lorenzo E, Esposito G, Pisani A, Leccia A, Cavuto L, Stingone AM, Chieffo A, et al. Effects of

- hydroxymethylglutaryl coenzyme A reductase inhibitor simvastatin on smooth muscle cell proliferation in vitro and neointimal formation in vivo after vascular injury. *J Am Coll Cardiol*. 2000;35:214–221. doi: [10.1016/S0735-1097\(99\)00526-4](https://doi.org/10.1016/S0735-1097(99)00526-4)
33. Tosch V, Rohde HM, Tronchere H, Zanoteli E, Monroy N, Kretz C, Dondaine N, Payrastra B, Mandel JL, Laporte J. A novel PtdIns3P and PtdIns(3,5)P2 phosphatase with an inactivating variant in centronuclear myopathy. *Hum Mol Genet*. 2006;15:3098–3106. doi: [10.1093/hmg/ddl250](https://doi.org/10.1093/hmg/ddl250)
  34. Jungbluth H, Wallgren-Pettersson C, Laporte J. Centronuclear (myotubular) myopathy. *Orphanet J Rare Dis*. 2008;3:26. doi: [10.1186/1750-1172-3-26](https://doi.org/10.1186/1750-1172-3-26)
  35. Shen J, Yu WM, Brotto M, Scherman JA, Guo C, Stoddard C, Nosek TM, Valdivia HH, Qu CK. Deficiency of MIP/MTMR14 phosphatase induces a muscle disorder by disrupting Ca(2+) homeostasis. *Nat Cell Biol*. 2009;11:769–776. doi: [10.1038/ncb1884](https://doi.org/10.1038/ncb1884)
  36. Yin L, Yong-Bo P, Meng-Fei Y, Weiwei C, Ping Z, Lu X, Li-Qun M, Congli C, Qing-Hua L, Jinhua S. Mice lacking myotubularin-related protein 14 show accelerated high-fat diet-induced lipid accumulation and inflammation. *J Physiol Biochem*. 2017;73:17–28. doi: [10.1007/s13105-016-0520-6](https://doi.org/10.1007/s13105-016-0520-6)
  37. Lv Y, Xue L, Cai C, Liu QH, Shen J. Deficiency of myotubularin-related protein 14 influences body weight, metabolism, and inflammation in an age-dependent manner. *Cell Biosci*. 2015;5:69. doi: [10.1186/s13578-015-0062-6](https://doi.org/10.1186/s13578-015-0062-6)
  38. Stoger JL, Gijbels MJ, van der Velden S, Manca M, van der Loos CM, Biessen EA, Daemen MJ, Lutgens E, de Winther MP. Distribution of macrophage polarization markers in human atherosclerosis. *Atherosclerosis*. 2012;225:461–468. doi: [10.1016/j.atherosclerosis.2012.09.013](https://doi.org/10.1016/j.atherosclerosis.2012.09.013)
  39. Hanna RN, Shaked I, Hubbeling HG, Punt JA, Wu R, Herrley E, Zaugg C, Pei H, Geissmann F, Ley K, et al. NR4A1 (Nur77) deletion polarizes macrophages toward an inflammatory phenotype and increases atherosclerosis. *Circ Res*. 2012;110:416–427. doi: [10.1161/CIRCRESAHA.111.253377](https://doi.org/10.1161/CIRCRESAHA.111.253377)
  40. Murphy AJ, Dragoljevic D, Tall AR. Cholesterol efflux pathways regulate myelopoiesis: a potential link to altered macrophage function in atherosclerosis. *Front Immunol*. 2014;5:490. doi: [10.3389/fimmu.2014.00490](https://doi.org/10.3389/fimmu.2014.00490)
  41. Bernhagen J, Krohn R, Lue H, Gregory JL, Zerneck A, Koenen RR, Dewor M, Georgiev I, Schober A, Leng L, et al. MIF is a noncognate ligand of CXC chemokine receptors in inflammatory and atherogenic cell recruitment. *Nat Med*. 2007;13:587–596. doi: [10.1038/nm1567](https://doi.org/10.1038/nm1567)
  42. Peled M, Fisher EA. Dynamic aspects of macrophage polarization during atherosclerosis progression and regression. *Front Immunol*. 2014;5:579. doi: [10.3389/fimmu.2014.00579](https://doi.org/10.3389/fimmu.2014.00579)
  43. Gomez D, Shankman LS, Nguyen AT, Owens GK. Detection of histone modifications at specific gene loci in single cells in histological sections. *Nat Methods*. 2013;10:171–177. doi: [10.1038/nmeth.2332](https://doi.org/10.1038/nmeth.2332)
  44. Wamhoff BR, Hoofnagle MH, Burns A, Sinha S, McDonald OG, Owens GK. A G/C element mediates repression of the SM22alpha promoter within phenotypically modulated smooth muscle cells in experimental atherosclerosis. *Circ Res*. 2004;95:981–988. doi: [10.1161/01.RES.0000147961.09840.fb](https://doi.org/10.1161/01.RES.0000147961.09840.fb)
  45. Rong JX, Shapiro M, Trogan E, Fisher EA. Transdifferentiation of mouse aortic smooth muscle cells to a macrophage-like state after cholesterol loading. *Proc Natl Acad Sci USA*. 2003;100:13531–13536. doi: [10.1073/pnas.1735526100](https://doi.org/10.1073/pnas.1735526100)
  46. Liu Z, Sun Q, Wang X. PLK1, a potential target for cancer therapy. *Transl Oncol*. 2017;10:22–32. doi: [10.1016/j.tranon.2016.10.003](https://doi.org/10.1016/j.tranon.2016.10.003)
  47. St-Denis N, Gupta GD, Lin ZY, Gonzalez-Badillo B, Pelletier L, Gingras AC. Myotubularin-related proteins 3 and 4 interact with polo-like kinase 1 and centrosomal protein of 55 kDa to ensure proper abscission. *Mol Cell Proteomics*. 2015;14:946–960. doi: [10.1074/mcp.M114.046086](https://doi.org/10.1074/mcp.M114.046086)
  48. Wilson JL, Wang L, Zhang Z, Hill NS, Polgar P. Participation of PLK1 and FOXM1 in the hyperplastic proliferation of pulmonary artery smooth muscle cells in pulmonary arterial hypertension. *PLoS One*. 2019;14:e0221728. doi: [10.1371/journal.pone.0221728](https://doi.org/10.1371/journal.pone.0221728)
  49. Rezey AC, Gerlach BD, Wang R, Liao G, Tang DD. Plk1 mediates paxillin phosphorylation (Ser-272), centrosome maturation, and airway smooth muscle layer thickening in allergic asthma. *Sci Rep*. 2019;9:7555. doi: [10.1038/s41598-019-43927-8](https://doi.org/10.1038/s41598-019-43927-8)
  50. de Carcer G, Wachowicz P, Martinez-Martinez S, Oller J, Mendez-Barbero N, Escobar B, Gonzalez-Loyola A, Takaki T, El Bakkali A, Camara JA, et al. Plk1 regulates contraction of postmitotic smooth muscle cells and is required for vascular homeostasis. *Nat Med*. 2017;23:964–974. doi: [10.1038/nm.4364](https://doi.org/10.1038/nm.4364)
  51. Kotian S, Zhang L, Boufraquech M, Gaskins K, Gara SK, Quezado M, Nilubol N, Kebebew E. Dual inhibition of HDAC and tyrosine kinase signaling pathways with CUDC-907 inhibits thyroid cancer growth and metastases. *Clin Cancer Res*. 2017;23:5044–5054. doi: [10.1158/1078-0432.CCR-17-1043](https://doi.org/10.1158/1078-0432.CCR-17-1043)
  52. Johnson GL, Lapadat R. Mitogen-activated protein kinase pathways mediated by ERK, JNK, and p38 protein kinases. *Science*. 2002;298:1911–1912. doi: [10.1126/science.1072682](https://doi.org/10.1126/science.1072682)
  53. Chen Z, Gibson TB, Robinson F, Silvestro L, Pearson G, Xu B, Wright A, Vanderbilt C, Cobb MH. MAP kinases. *Chem Rev*. 2001;101:2449–2476. doi: [10.1021/cr000241p](https://doi.org/10.1021/cr000241p)
  54. Gadang V, Konanah E, Hui DY, Jaeschke A. Mixed-lineage kinase 3 deficiency promotes neointima formation through increased activation of the RhoA pathway in vascular smooth muscle cells. *Arterioscler Thromb Vasc Biol*. 2014;34:1429–1436. doi: [10.1161/ATVBAHA.114.303439](https://doi.org/10.1161/ATVBAHA.114.303439)
  55. Proctor BM, Jin X, Lupu TS, Muglia LJ, Semenkovich CF, Muslin AJ. Requirement for p38 mitogen-activated protein kinase activity in neointima formation after vascular injury. *Circulation*. 2008;118:658–666. doi: [10.1161/CIRCULATIONAHA.107.734848](https://doi.org/10.1161/CIRCULATIONAHA.107.734848)
  56. Kume M, Komori K, Matsumoto T, Onohara T, Takeuchi K, Yonemitsu Y, Sugimachi K. Administration of a decoy against the activator protein-1 binding site suppresses neointimal thickening in rabbit balloon-injured arteries. *Circulation*. 2002;105:1226–1232. doi: [10.1161/hc1002.104903](https://doi.org/10.1161/hc1002.104903)
  57. Gennaro G, Menard C, Michaud SE, Deblois D, Rivard A. Inhibition of vascular smooth muscle cell proliferation and neointimal formation in injured arteries by a novel, oral mitogen-activated protein kinase/extracellular signal-regulated kinase inhibitor. *Circulation*. 2004;110:3367–3371. doi: [10.1161/01.CIR.0000147773.86866.CD](https://doi.org/10.1161/01.CIR.0000147773.86866.CD)
  58. Wang HB, Huang SH, Xu M, Yang J, Yang J, Liu MX, Wan CX, Liao HH, Fan D, Tang QZ. Galangin ameliorates cardiac remodeling via the MEK1/2-ERK1/2 and PI3K-AKT pathways. *J Cell Physiol*. 2019;234:15654–15667. doi: [10.1002/jcp.28216](https://doi.org/10.1002/jcp.28216)
  59. Pei H, Wang W, Zhao D, Su H, Su G, Zhao Z. G protein-coupled estrogen receptor 1 inhibits angiotensin II-induced cardiomyocyte hypertrophy via the regulation of PI3K-Akt-mTOR signalling and autophagy. *Int J Biol Sci*. 2019;15:81–92. doi: [10.7150/ijbs.28304](https://doi.org/10.7150/ijbs.28304)
  60. Li J, Yuan YP, Xu SC, Zhang N, Xu CR, Wan CX, Ren J, Zeng XF, Tang QZ. Arctiin protects against cardiac hypertrophy through inhibiting MAPKs and AKT signaling pathways. *J Pharmacol Sci*. 2017;135:97–104. doi: [10.1016/j.jphs.2017.05.012](https://doi.org/10.1016/j.jphs.2017.05.012)
  61. Abeyathna P, Su Y. The critical role of Akt in cardiovascular function. *Vascul Pharmacol*. 2015;74:38–48. doi: [10.1016/j.vph.2015.05.008](https://doi.org/10.1016/j.vph.2015.05.008)
  62. Yu C, Luo D, Yu J, Zhang M, Zheng X, Xu G, Wang J, Wang H, Xu Y, Jiang K, et al. Genome-wide CRISPR-cas9 knockout screening identifies GRB7 as a driver for MEK inhibitor resistance in KRAS mutant colon cancer. *Oncogene*. 2022;41:191–203. doi: [10.1038/s41388-021-02077-w](https://doi.org/10.1038/s41388-021-02077-w)

## **SUPPLEMENTAL MATERIAL**

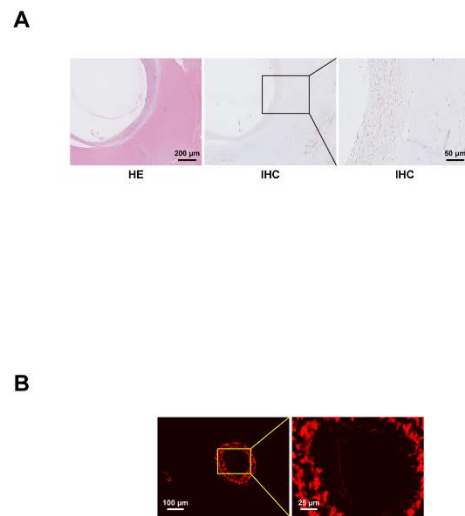
**Table S1. Primers**

| Gene name | Forward primer (mouse)  | Reverse primer (mouse)   |
|-----------|-------------------------|--------------------------|
| MTMR14    | CCACATCGTATTCCTGGAGTAT  | AGACAAACCGACCTCTGCAC     |
| PCNA      | TTTGAGGCACGCCTGATCC     | GGAGACGTGAGACGAGTCCAT    |
| ACTA2     | GTCCCAGACATCAGGGAGTAA   | TCGGATACTTCAGCGTCAGGA    |
| MTMR1     | AAGAACAGCGAAAACCTGGGA   | TGGCAGGATAGGTATCACAGAAC  |
| MTMR2     | AGAACTCGGTGCATACCAAATC  | GCTAACTTGTTTGCCTCCCTCA   |
| MTMR3     | ATGACTCGTTGGCTACCTGAC   | GAACCGGAACCTTCTGGTTAC    |
| MTMR4     | AAAGACTCTGTCATCAACGTGC  | CCGGCTTAGCCTTGAGAGC      |
| MTMR5     | TGGTTACCACCACACATCCC    | CCCTGCGTTCACCCTTCTC      |
| MTMR6     | ACAGGAACACTGTATCTTACGGC | AAGTGGTCAGAGCAAGTTTCTC   |
| MTMR7     | GTGGAAGAATCGAGCTGACTAC  | CCCCTTTTCAAAGCGGTTATAACA |
| MTMR9     | ATGGAGTTTGCGGAGCTGATT   | GATGGCGTCGATATTTGAATGGA  |
| MTMR10    | TTATTCCCAGCCAACAGACCT   | CACCTCCTGAGGATACTCCATT   |
| MTMR11    | CCTGGCCTCTGGTTGTCTC     | GTATCCTGCTTTTCGCTGCCAT   |
| MTMR12    | GCCAGCACAGTCCTGAAGTAT   | GCTTCCCCGCCATTATCCAG     |
| MTMR13    | TGGTGGAAAAAGCGTGTTTCA   | GCATAGCGAATACAGCCTGTT    |
| MTMR15    | ATGCCGTCACAAAGGAAATCA   | ATGCAAGTTTAGCAGGTGGTG    |
| 18S       | GTAACCCGTTGAACCCCAT     | CCATCCAATCGGTAGTAGCG     |

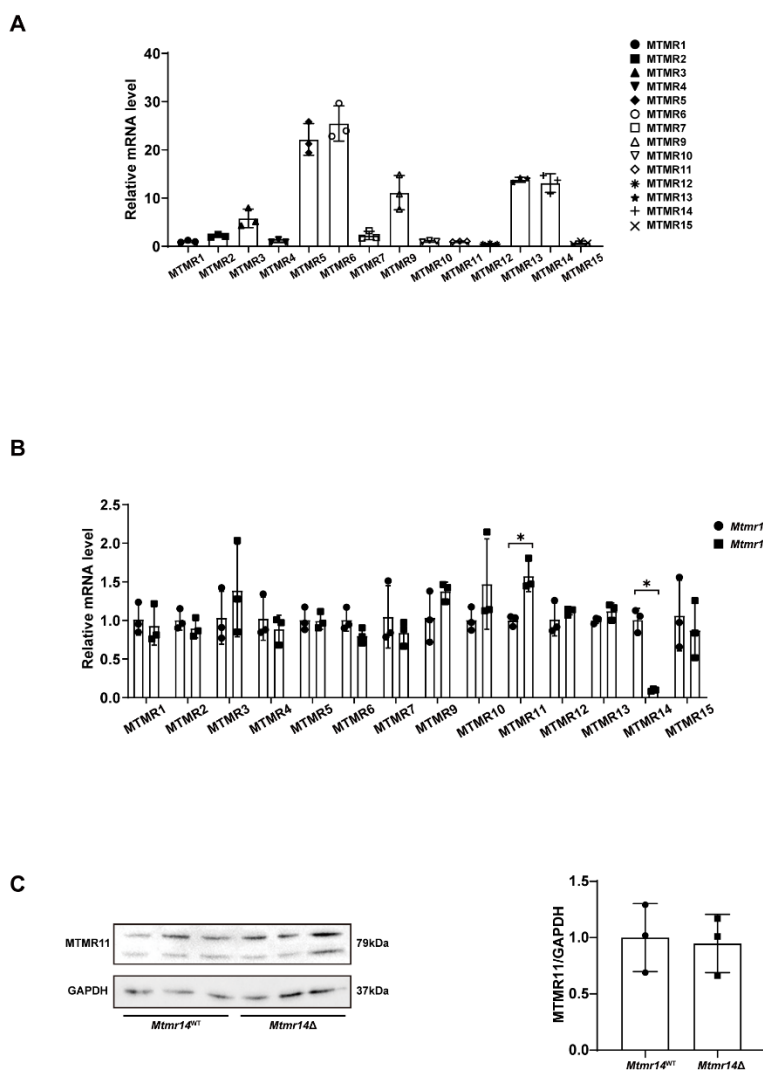
| Gene name | Forward primer (rat) | Reverse primer (rat) |
|-----------|----------------------|----------------------|
| MTMR14    | AGTCACTCATCCTCCCCACA | GTCTCCCTGTCACTCAGAGC |
| 18S       | GTAACCCGTTGAACCCCAT  | CCATCCAATCGGTAGTAGCG |

**Figure S1. Myotubularin-related protein 14 (MTMR14) was concentrated in the neointima of human restenosis artery.**



**A.** Representative images of hematoxylin-eosin (HE) and immunohistochemistry (IHC) staining with an anti-MTMR14 antibody in slices from human restenosis artery (scale bar, 200 μm); **B.** Zoom-in image of ACTA2 immunofluorescence (IF) staining in the mouse carotid artery ligation (CAL) model (scale bar, 100μm).

**Figure S2. Isoenzymes of myotubularin-related (MTMR) phosphatase expression in vascular smooth muscle cells (VSMCs) and the compensation for expression of isoenzymes when knockdown myotubularin-related protein 14 (MTMR14).**

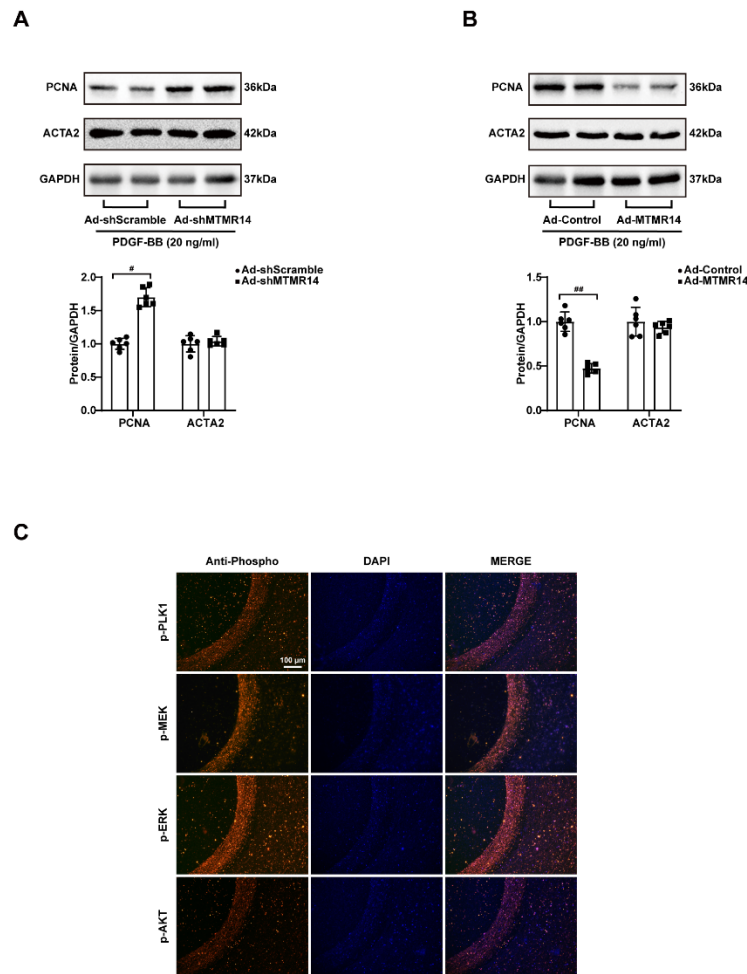


**A.** Representative mRNA levels of isoenzymes of MTMR phosphatase expressed in vascular smooth muscle cells (n=3); **B.** Representative mRNA levels of isoenzymes of MTMR phosphatase expressed after MTMR14 knockdown (n=3); **C.** Representative protein levels of myotubularin-related protein 11 (MTMR11) after MTMR14 knockdown (n=3). (\* $p < 0.05$  *Mtmr14* $\Delta$  versus *Mtmr14*<sup>WT</sup>)

**Figure S3. Results of liquid chromatography-tandem mass spectrometry (LC-MS/MS) analysis.**

| Unused | %Cov(95) | Accession | Gene    | Peptides(9) | Spectra |
|--------|----------|-----------|---------|-------------|---------|
| 21.39  | 20.07    | P53350    | PLK1    | 10          | 10      |
| 8.67   | 8.769    | Q8NCE2    | MTMR14  | 5           | 6       |
| 7.08   | 9.719    | P61978    | HNRNPK  | 4           | 4       |
| 6.89   | 7.741    | O43390    | HNRNPR  | 3           | 3       |
| 4.86   | 6.238    | Q9Y2X3    | NOP58   | 2           | 2       |
| 4.04   | 5.38     | P50991    | CCT4    | 2           | 2       |
| 3.72   | 5.36     | P48643    | CCT5    | 2           | 2       |
| 2.16   | 1.868    | P14866    | HNRNPL  | 1           | 1       |
| 2      | 2.946    | Q9NZI8    | IGF2BP1 | 1           | 1       |
| 2      | 4.049    | P07477    | PRSS1   | 2           | 3       |
| 2      | 1.525    | Q02413    | DSG1    | 1           | 1       |
| 2      | 2.19     | O15371    | EIF3D   | 1           | 1       |
| 2      | 2.662    | P35637    | FUS     | 1           | 1       |
| 1.85   | 1.766    | P36957    | DLST    | 1           | 1       |
| 1.72   | 3.326    | P68363    | TUBA1B  | 1           | 1       |
| 1.38   | 1.132    | P23246    | SFPQ    | 1           | 1       |
| 1.35   | 3.16     | Q07666    | KHDRBS1 | 1           | 1       |

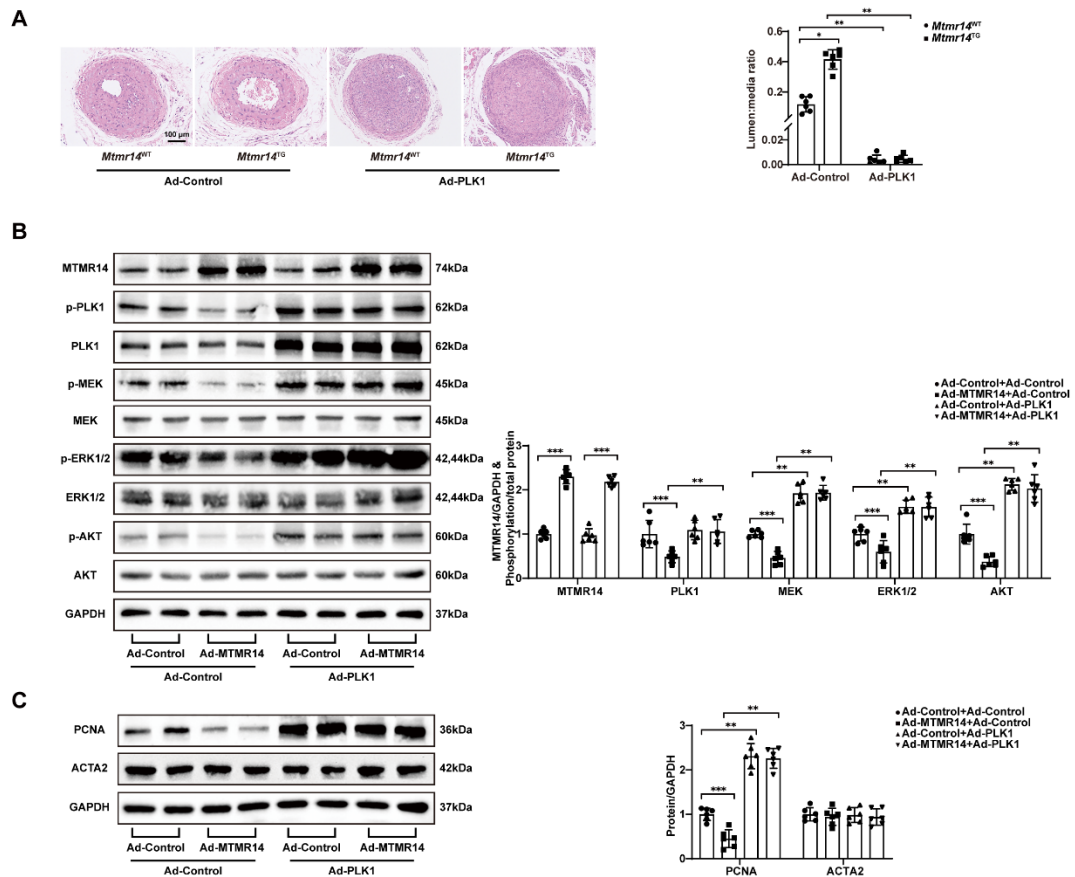
**Figure S4. Manipulation of myotubularin-related protein 14 (MTMR14) did not affect the contraction of vascular smooth muscle cell (VSMC) but did affect the proliferation of VSMC.**



**A.** Western blot assays were performed in primary VSMCs infected with Ad-shScramble or Ad-shMTMR14 at 24 hours after platelet-derived growth factor BB (PDGF-BB) stimulation to detect the expression of PCNA and ACTA2; **B.** Western blot assays were performed in primary VSMCs infected with Ad-Control or Ad-MTMR14 at 24 hours after PDGF-BB stimulation to detect the expression of PCNA and ACTA2. **C.** Representative images of immunofluorescence staining of p-PLK1/p-MEK/p-ERK/p-AKT in slices from human restenosis artery (scale bar, 100  $\mu$ m). (GAPDH served as the loading control,  $n=6$ ,  $\#p < 0.05$  versus Ad-shScramble,  $##p < 0.05$  versus Ad-Control)



**Figure S5. The overexpression of polo-like kinase 1 (PLK1) could aggravate the phenotype induced by myotubularin-related protein 14 (MTMR14) overexpression *in vivo* and *in vitro*.**



**A.** Representative hematoxylin-eosin (HE) staining images of carotid arteries from *Mtmr14<sup>WT</sup>* or MTMR14-transgenic (*Mtmr14<sup>TG</sup>*) mice local infected with Ad-Control or Ad-PLK1 at 28 days after ligation (scale bar, 100  $\mu$ m; n=6); **B-C.** Western blot assays were performed in primary VSMCs infected with Ad-Control+ Ad-Control, Ad-MTMR14+ Ad-Control, Ad-Control+Ad-PLK1 or Ad-MTMR14+Ad-PLK1 after 20ng/ml platelet-derived growth factor BB (PDGF-BB) stimulation for 24 hours to detect the expression of PLK1, p-PLK1, MEK, p-MEK, ERK1/2, p-ERK1/2, AKT, p-AKT, PCNA and ACTA2 (GAPDH served as the loading control, n=6). (\* $p$  < 0.05 *Mtmr14<sup>TG</sup>* versus *Mtmr14<sup>WT</sup>*, \*\* $p$  < 0.05 Ad-PLK1 versus Ad-

Control, \*\*\* $p < 0.05$  Ad-MTMR14 versus Ad-Control)